Models and Simulations of Single and Shattered Pellet Ablation

Roman Samulyak, *Stony Brook University*

Nicholas Bosviel, Xingyu Wang *(supported PhD students, SBU)*

Paul Parks, *Consultant, General Atomics*

Talk Overview

- Physics Models
  - EOS
  - Conductivity
  - Radiation
- Simulations of single pellet injection
  - Verification of Scaling laws
  - MHD effects
- Progress on simulation of SPI
  - 3D Lagrangian Particle code for multiple pellet fragments

Physics Models for Pellet Simulations

- Kinetic model for the interaction of hot electrons with ablated gas

- Explicitly tracked pellet surface
- Phase transition (ablation model)

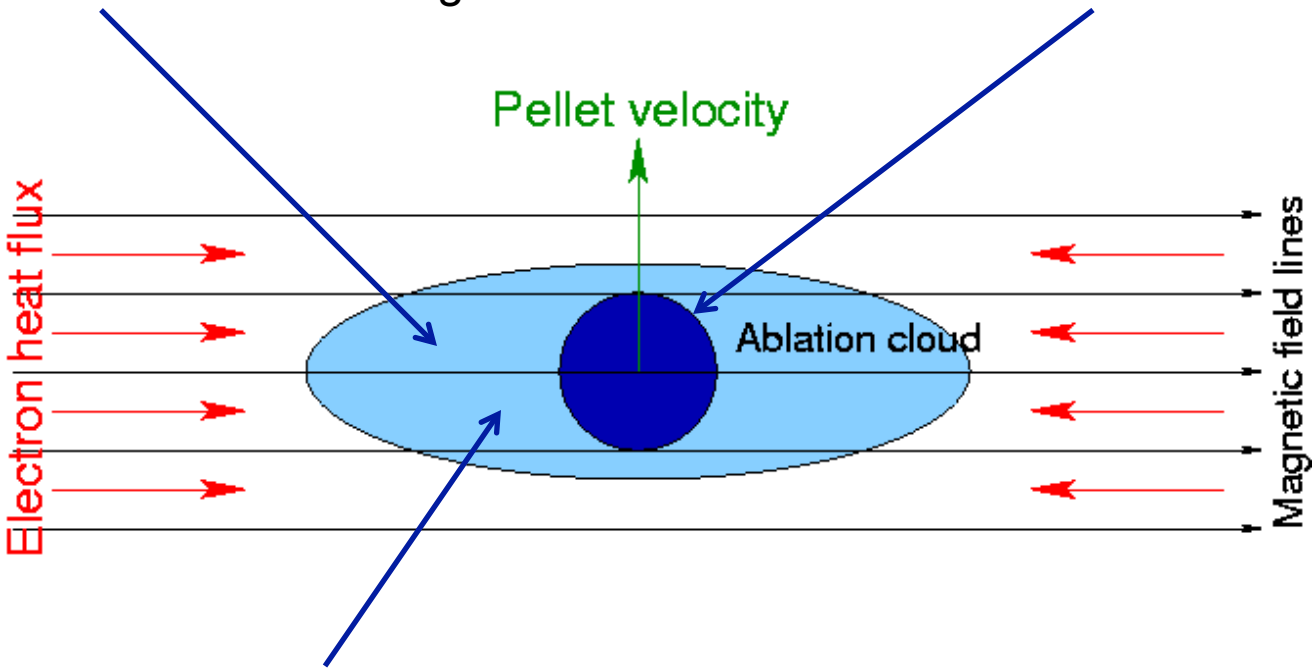

- Low Magnetic Re MHD equations
- Equation of state with atomic processes
- Radiation model
- Conductivity models
- Pellet cloud charging models

Update on Physics Models

LTE EOS for high-Z materials: Saha equations

$$\frac{n_{m+1}n_e}{n_m} = 2\frac{u_{m+1}}{u_m}\left(\frac{2\pi m_e kT}{\eta^2}\right)^{3/2}\exp\left(-\frac{I_{m+1}}{kT}\right) = K_{m+1}(T)$$

$$\frac{f_{m+1}f_e}{f_m} = \frac{1}{\rho N}K_{m+1}(T)$$

$$P = N\rho\left(1+f_e\right)kT$$

$$E = \frac{3}{2}N(1+f_e)kT + N\sum_m Q_m f_m + N\sum_m W_m f_m,$$

- Fully coupled system of nonlinear equations
- Difficult to solve in each point at each time step of a hydro code

EOS for high-Z materials: continuum approximation

- Further development of ideas by Zeldovich
- Continuum approximation:

$$n_m \to n(m), \quad I_m \to I(m)$$

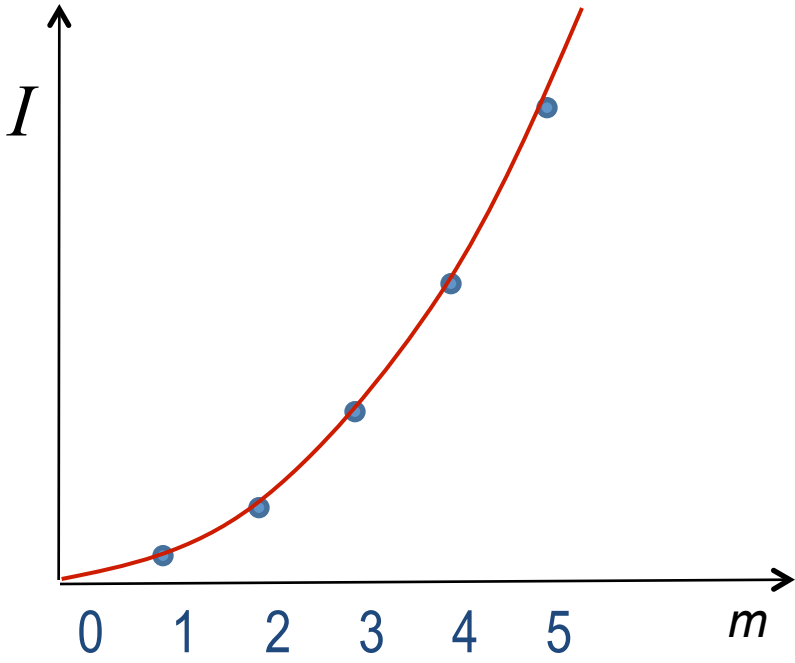

Conservation laws become

$$\int n(m)dm = n, \quad \int mn(m)dm = n_e$$

The system of Saha equations becomes an ODE

$$\left(1 + \frac{d\ln n}{dm}\right) n_e = AT^{3/2} \exp\left(-\frac{I(m+1)}{kT}\right)$$

For the average ionization, *dn/dm* = 0, and

$$\overline{m} = \frac{AT^{3/2}}{n} \exp\left(-\frac{\bar{I}}{kT}\right)$$

Verification of Zeldovich EOS model

- Very good agreement with coupled Saha equations for large ionization numbers
- There are questions whether the averaged ionization model is accurate for low Z
  - Using statistical weights, we were able to improve the agreement
  - The EOS is sufficiently accurate for hydro simulations from low to high Z

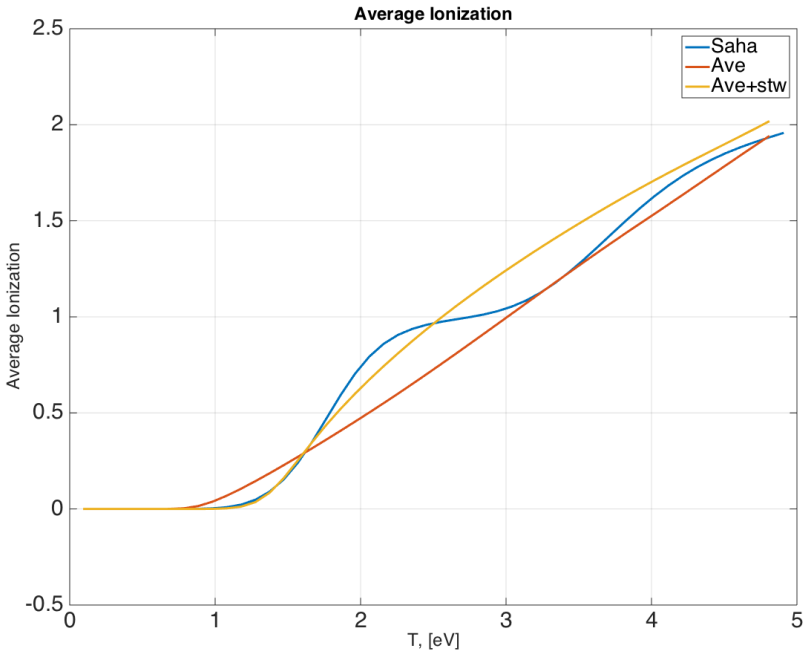

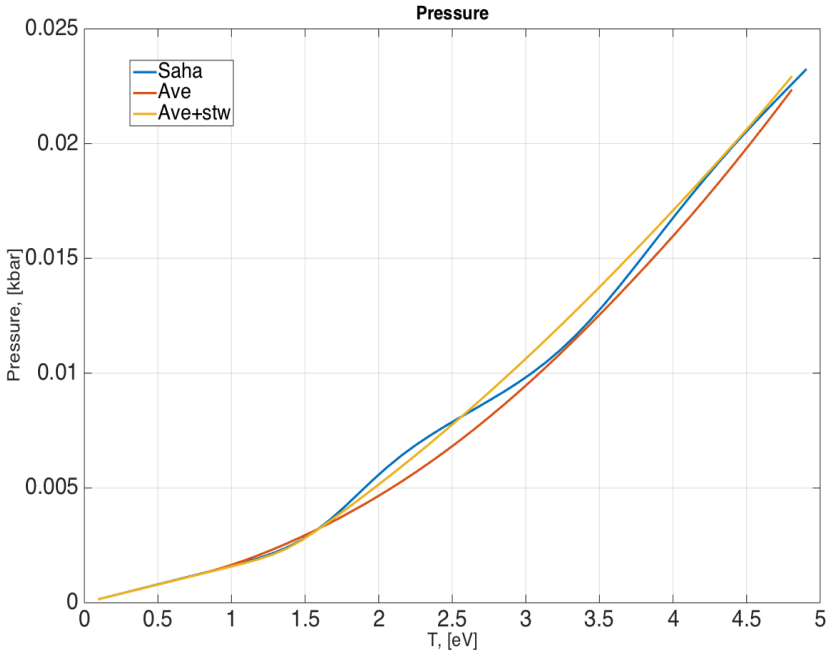

Non-ideal gas EOS

- In a thin layer near pellet surface, ideal EOS may not be accurate

- **Redlich-Kwong EOS** for cold and dense gas

$$P = \frac{RT}{V_m - b} - \frac{a}{T^{1/2} V_m \left(V_m - b\right)}$$

$$\text{where} \quad a = \frac{0.42748 R^2 T_{crit}^{5.2}}{P_{crit}}$$

$$b = \frac{0.08664 R T_{crit}}{P_{crit}}$$

• We have derived the complete EOS (expressions for entropy, sound speed, Gruneisen gamma etc.)

• Somewhat similar EOS (Peng-Robinson EOS), recommended by GA collaborators, contains empirical terms.

  • The derivation of complete EOS is problematic

  • Performing EOS plots in pellet-related range of parameters, we showed that PR EOS is practically identical to RK EOS.

• Implemented RK in FronTier and coupled to WENO solvers

Non-ideal EOS model: Results

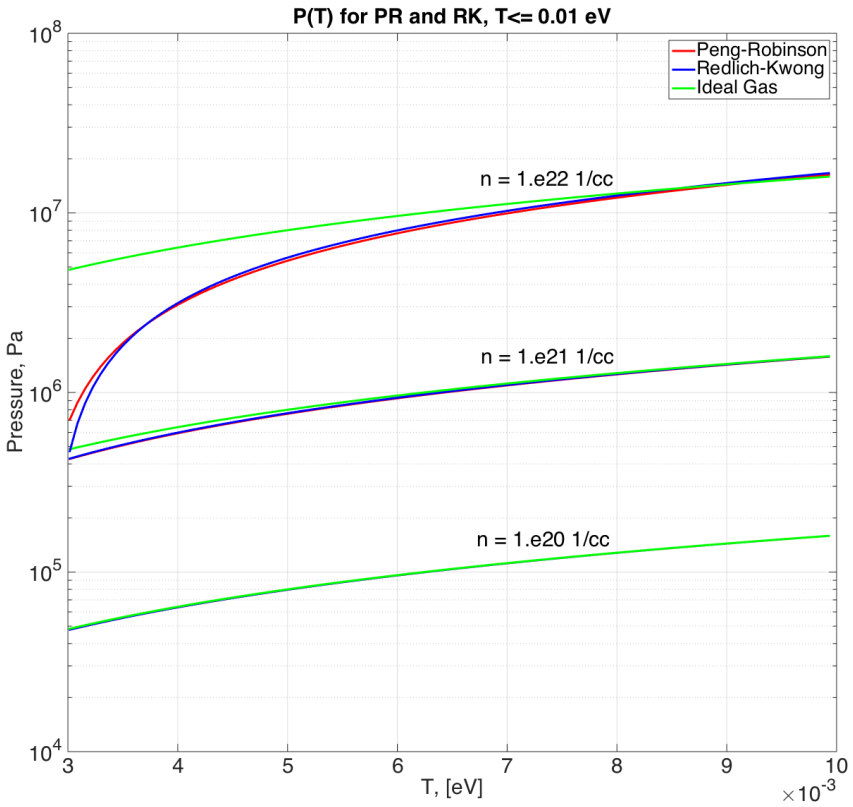

- RK and PR EOS models deviate from the ideal model only for densities larger than 1.e22 1/cc and T lower than 0.01 eV
- RK and PR EOS are practically identical

- Performed pellet simulations and showed that it has negligibly small effect on pellet ablation properties compared to the ideal EOS model

Radiation models

The photon mean free path in the ablation channel is much longer compared to the channel diameter and length

- The exception is the narrow region near the pellet surface, but the radiation coming from this region is very low
- Radiation model in thin optical limit is a good approximation

Two models were compared in our simulations:

- Radiation model based on **Jensen's theory** [R.V. Jensen et al, Nucl. Fusion, 17 (1977), 1187] (P. Parks provided tabulated data)

- Radiation model implemented in software from Prism Computational Sciences (**PROPACEOUS tables**)

$$\frac{de}{dt} = -4\sigma T_e^4 \chi_{Plank}$$

χ_{Plank} is Plank's emission opacity
PROPACEOS tables provide this in tabular form

Comparison of Radiation Models

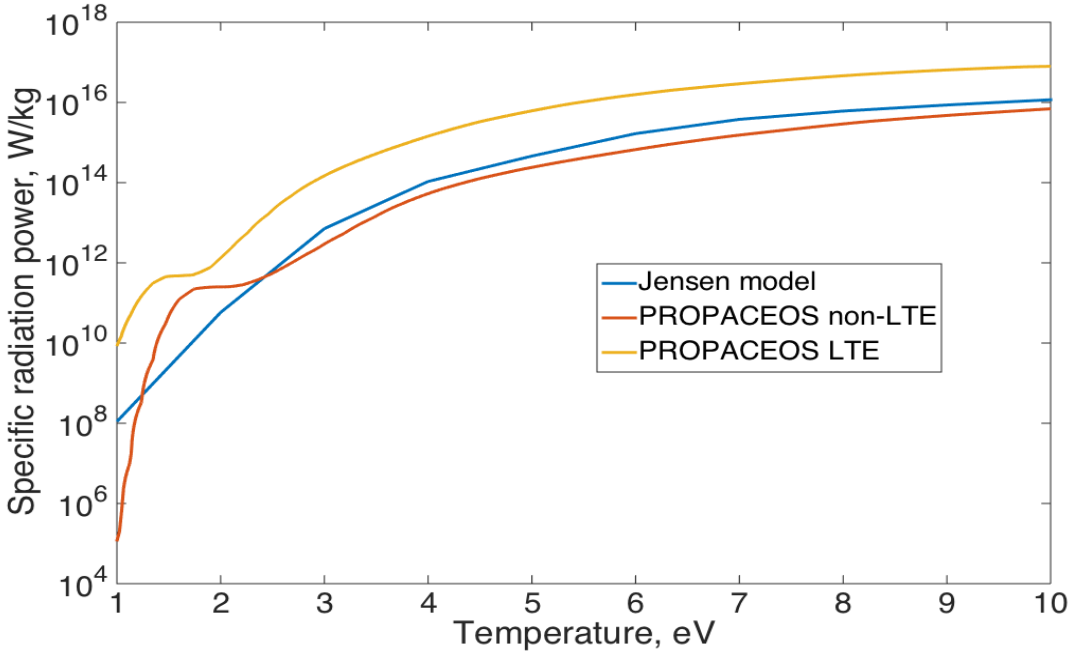

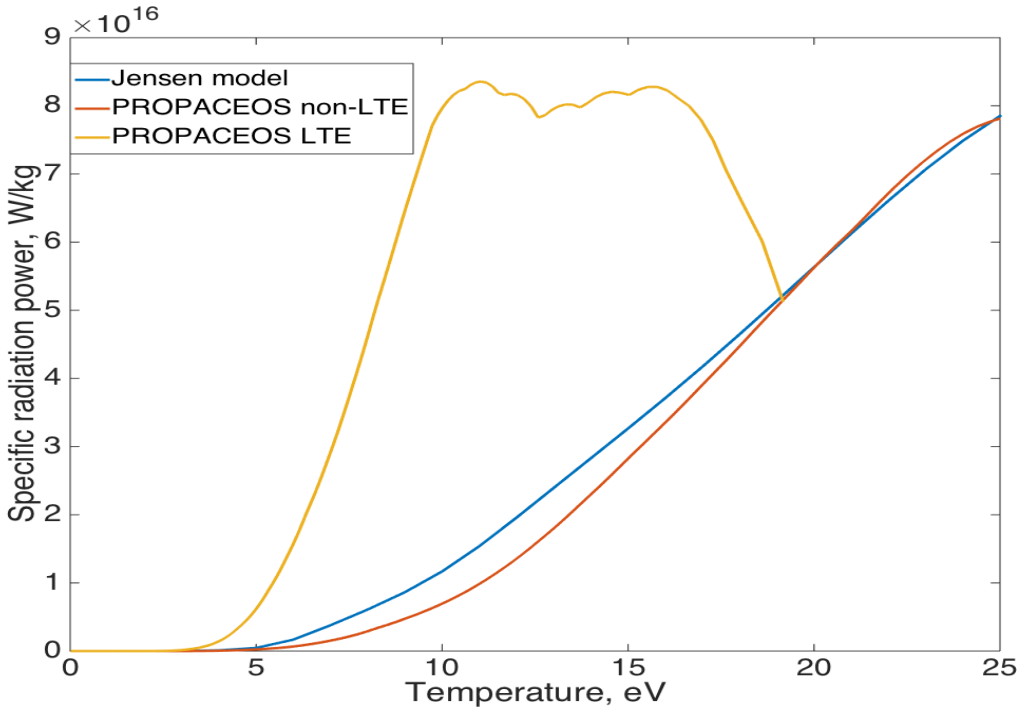

Radiation Models: Conclusions

- Jensen radiation model is very close to PROPACEOUS non-LTE table
- PROPACEOSU LTE tables give orders of magnitude higher radiation
- Our models currently used Jensen radiation model

- There is also a difference between LTE and non-LTE EOS

- Current simulations use the Jensen radiation model
- An obvious inconsistency in simulations:
  - LTE EOS model + non-LTE radiation model
  - Two different averaged ionization numbers: one found from Zeldovich LTE equations and the other one from data table

- Do we need to use non-LTE EOS?
  - Consistent simulations using PROPACEOUS non LTE EOS and radiation models?
  - Using **Z** from non-LTE Jensen radiation model?
  - Other ideas?

Electric conductivity model for high-Z materials

P. Parks (Jan. 2017)

$$\sigma_{\perp} = \frac{9700 T_e^{3/2}}{\left(Z_{eff} \ln \Lambda_{ei} + 0.00443 T_e^{2.245} \frac{n^0}{n_e} \right)}$$

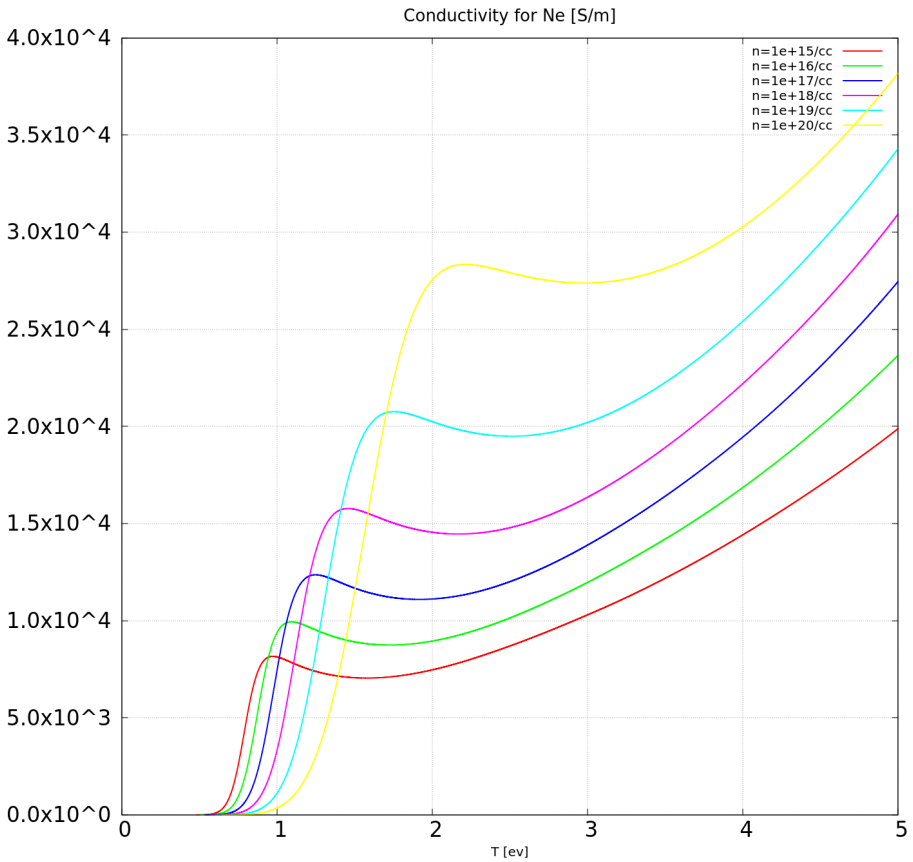

Verification: Comparison of Spherically Symmetric Simulations with Theory

- Spherically symmetric, no ionization, Maxwellian heat flux

$$G^{fit} = 67.08\left(\frac{T_e}{2000}\right)^{5/3}\left(\frac{r_p}{0.2}\right)^{4/3} n_{e14}^{1/3}$$

- units: $G(\mathrm{g/s}) \quad T_e(\mathrm{eV}) \quad r_p(\mathrm{cm}) \quad n_e(10^{14}\mathrm{cm}^{-3})$

- Surface recession speed

$$\frac{dr_p}{dt} = -\frac{G}{4\pi r_p^2 \rho_0} \quad (\mathrm{cm/s}) \qquad \rho_0 = 1.444 \ \ g/\mathrm{cm}^3$$

- Example: $G^{fit} = 26.621 \quad for \quad r_p = 0.1, n_{e14} = 1, T_e = 2000$
  which is close to the Parks numerical transonic flow value G = 25.5 and updated analytic scaling expression G = 26.56

Ne pellet baseline case, no atomic processes, previous results

$$\gamma = 5/3,\ r_p = 2\ \text{mm},\ T_{e\infty} = 2\ \text{keV},\ n_{e\infty} = 10^{14}\ \text{cm}^{-3}$$

Case	G (g/s)	T_* (eV)	r_* (mm)	P_{sur}/p_*
Semi-analytic	109.05	29.4167	5.858	6.478
FronTier	112.8	30.11	6.025	6.44

Ar pellet baseline case, no atomic processes

Case	G (g/s)	T_* (eV)	r_* (mm)	P_{sur}/p_*
Semi-analytic	103.1	61.59	5.858	6.47796
FronTier	103.8	61.81	5.877	6.3046

Ne pellet, electrostatic shielding effects, no atomic processes

$$\gamma = 5/3,\ r_p = 2\ \text{mm},\ T_{e\infty} = 2\ \text{keV},$$

$$n_{e\infty} = 10^{14}\ \text{cm}^{-3}\ ,\ n_{eff} = 1.068 \times 10^{13}\ \text{cm}^{-3}$$

Case	G (g/s)	T_* (eV)	p_* (bar)
Semi-analytic	51.74	6.623	5.858
FronTier	52.6	6.69	5.21

Ar pellet, electrostatic shielding effects, no atomic processes

Case	G (g/s)	T_* (eV)	p_* (bar)
Semi-analytic	47.33	12.98	4.76
FronTier	45.1	12.79	4.79

Verification of Scaling Laws for Ne Pellet (new results)

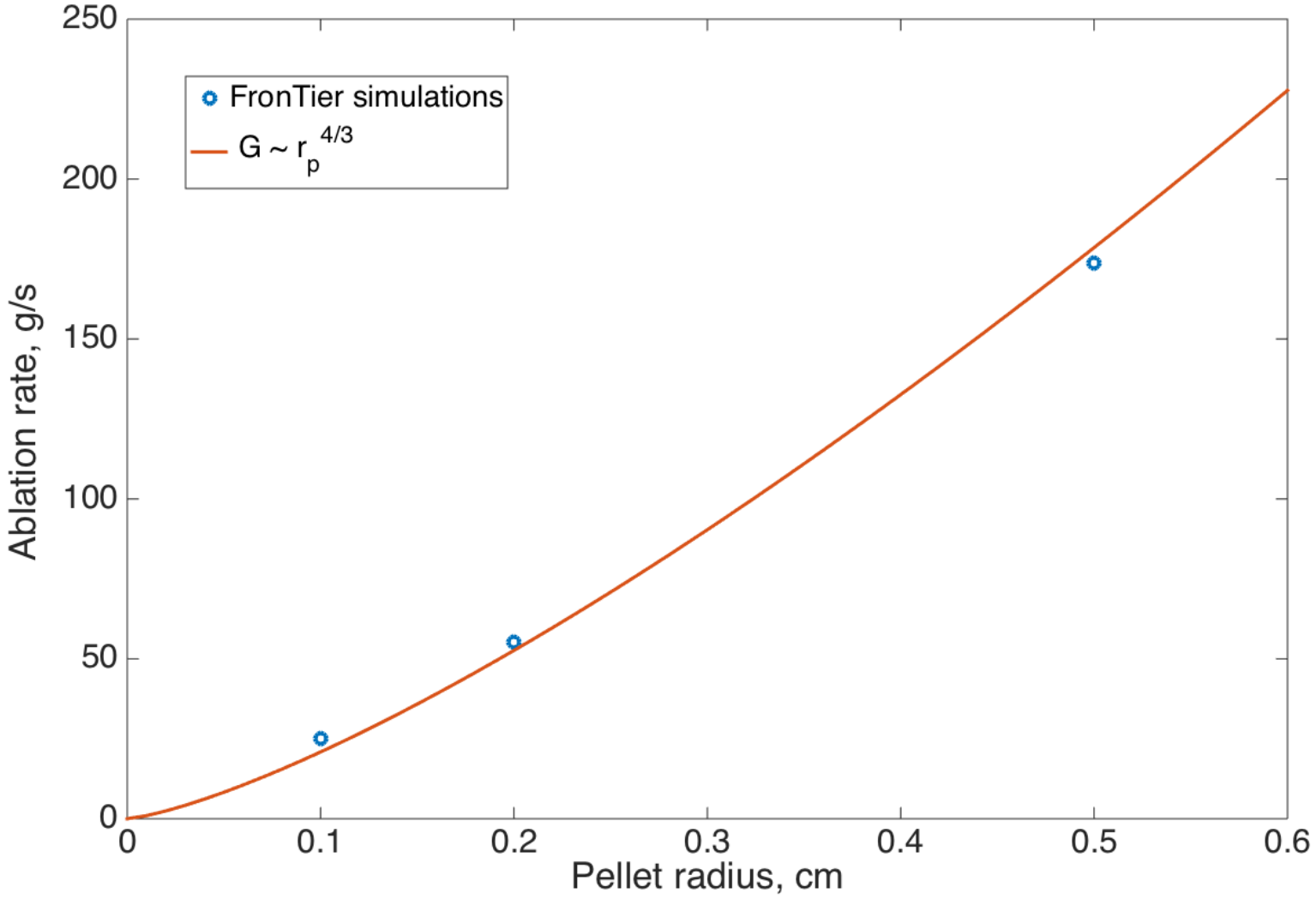

Verification of Scaling Laws for Ne Pellet

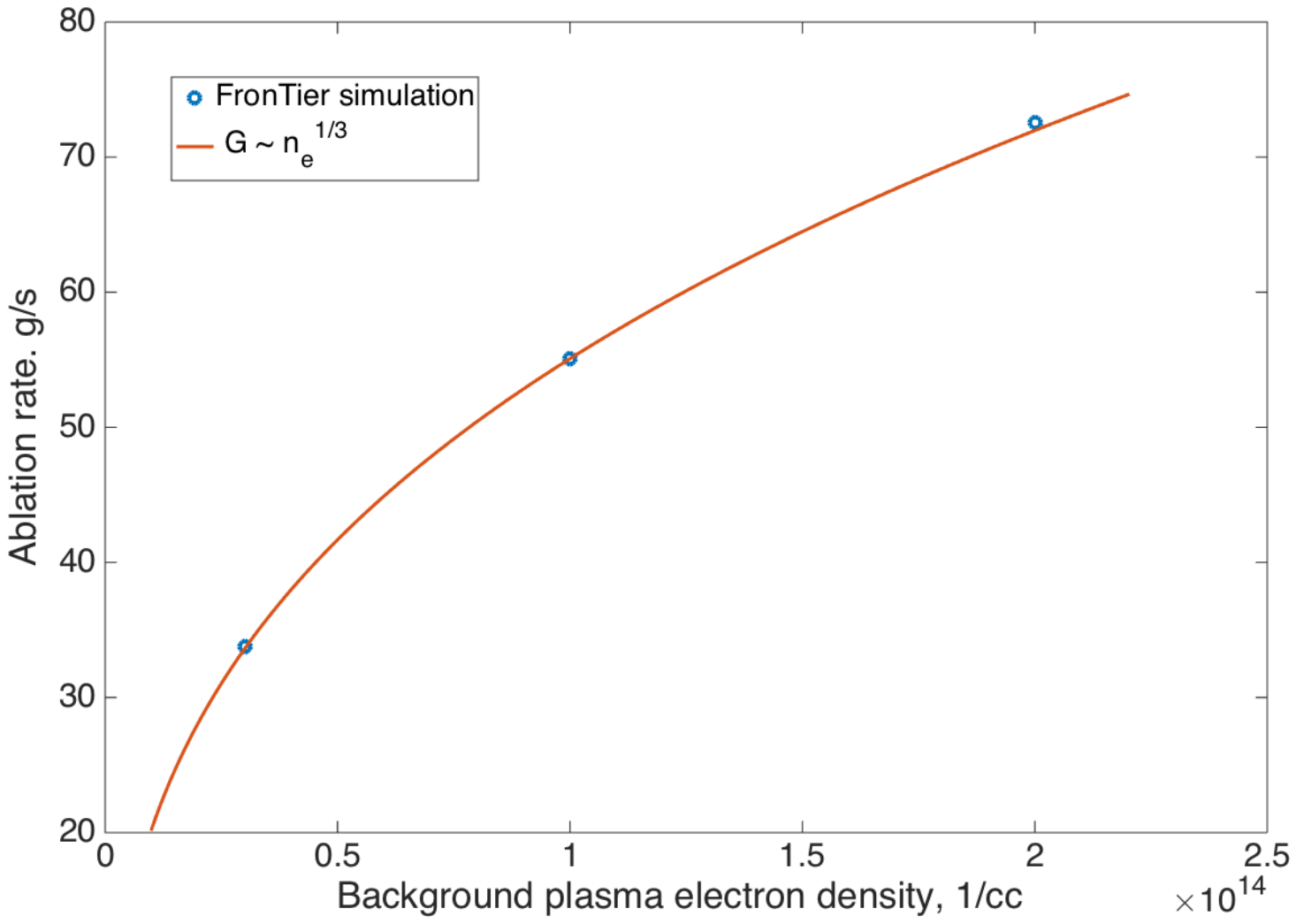

Verification of Scaling Laws for Ne Pellet

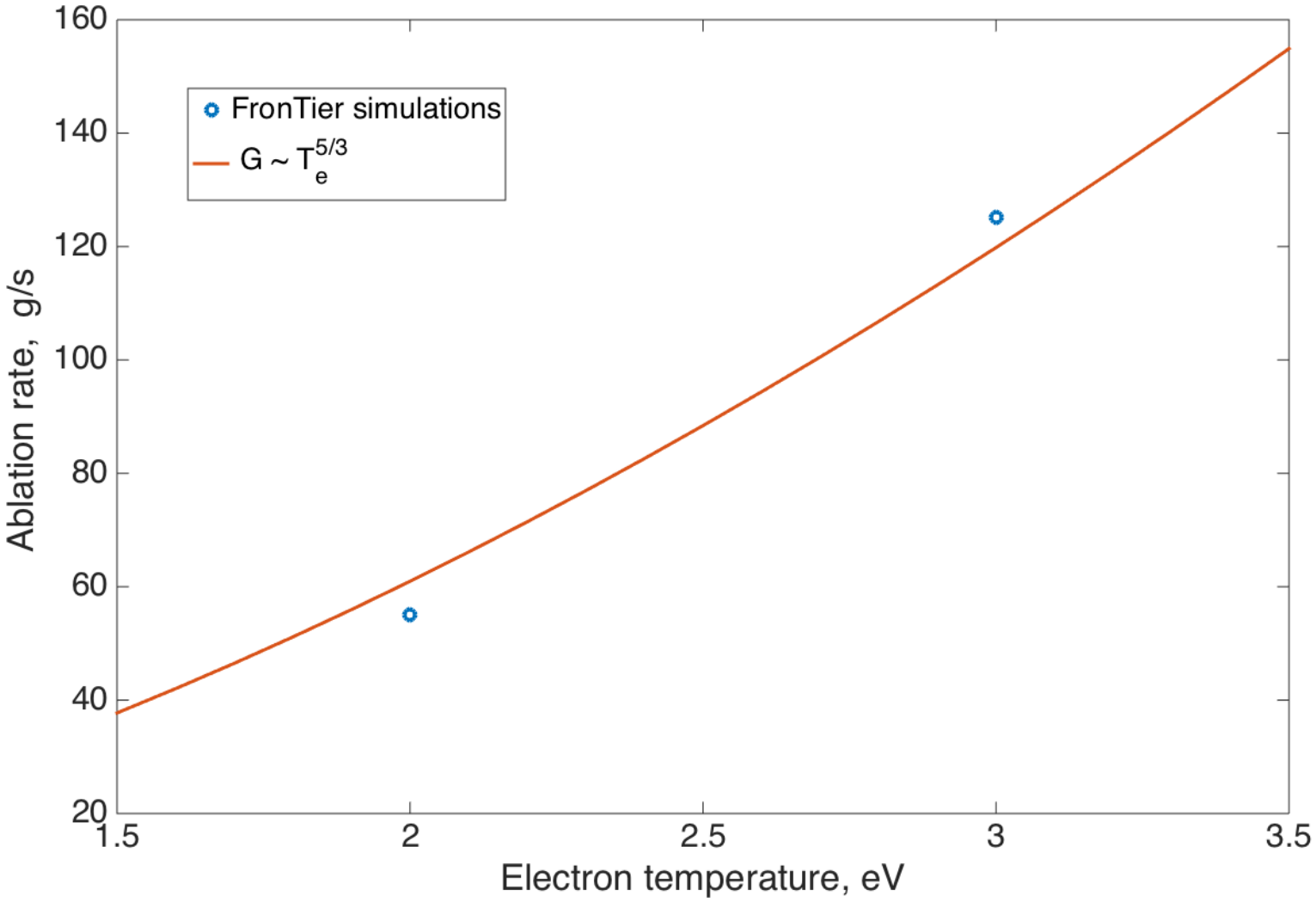

Influence of additiobal physics models

- Redlich-Kwong EOS has negligibly small effect on all processes
- Including atomic processes significantly changes the pressure and temperature, but the ablation rate was changed by only 4 % (no MHD)

Cylindrically symmetric MHD simulations

Simulation Parameters:

- Background electron density: 1.e14 1/cc – electrostatic shielding
- Electron Temperature: 2 keV
- Pellet radius: 2 mm
- “Warm-up time” (time during which the pellet crosses the pedestal: 10 microseconds
- Magnetic field: 6T
- MHD in low magnetic Reynolds number approximation
- No artificial “channel length”, which was imposed in our earlier DT simulations

Density, Temperature, Average Ionization at 1 microsecond

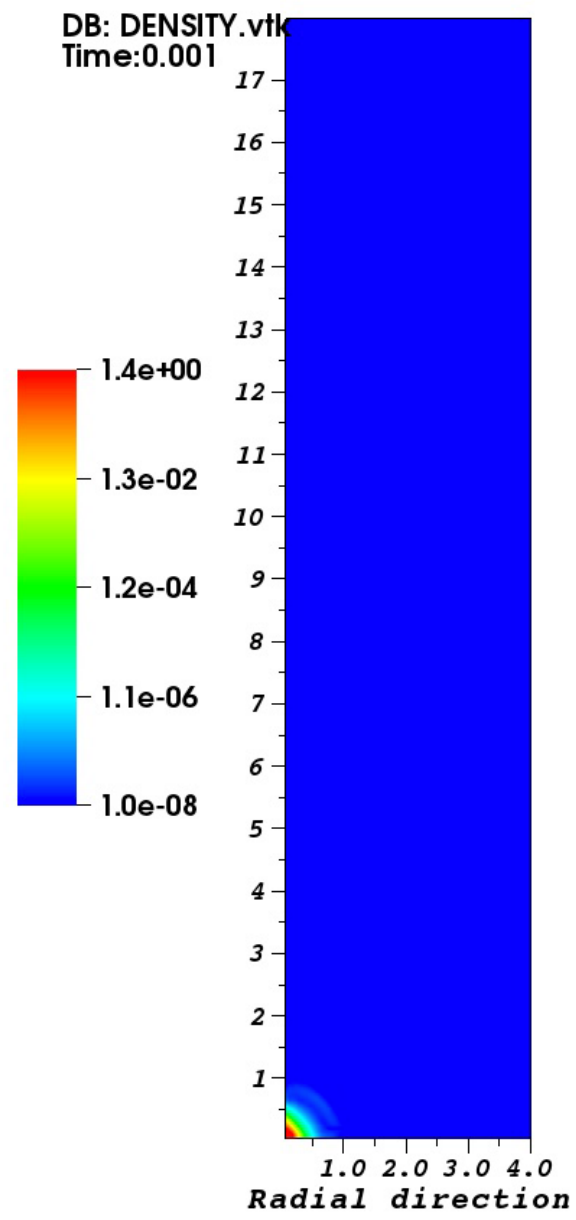

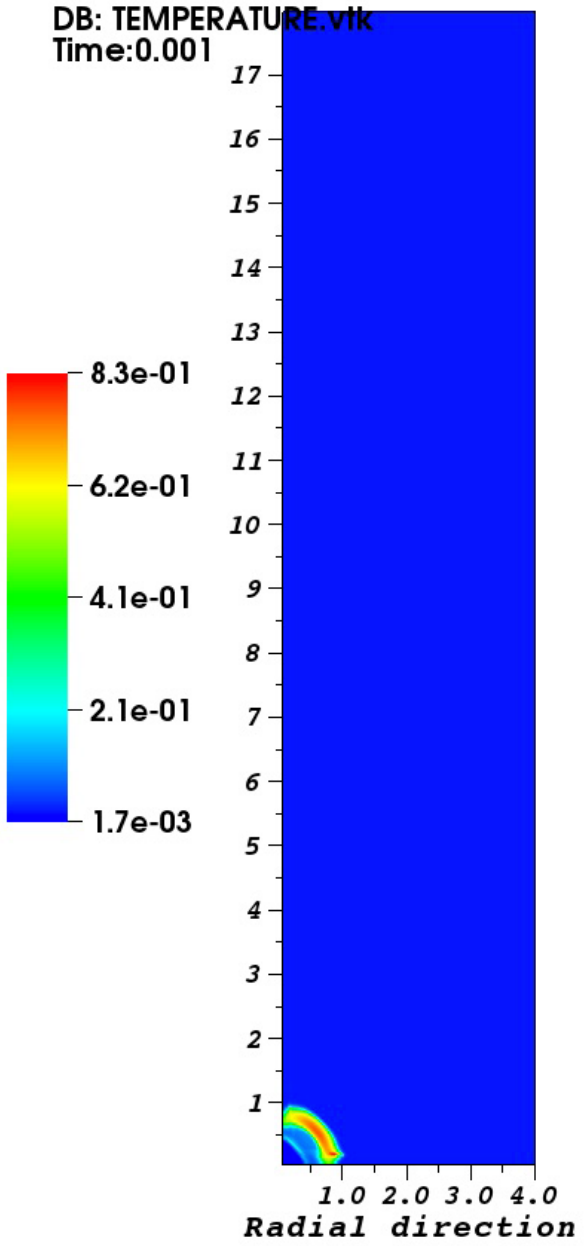

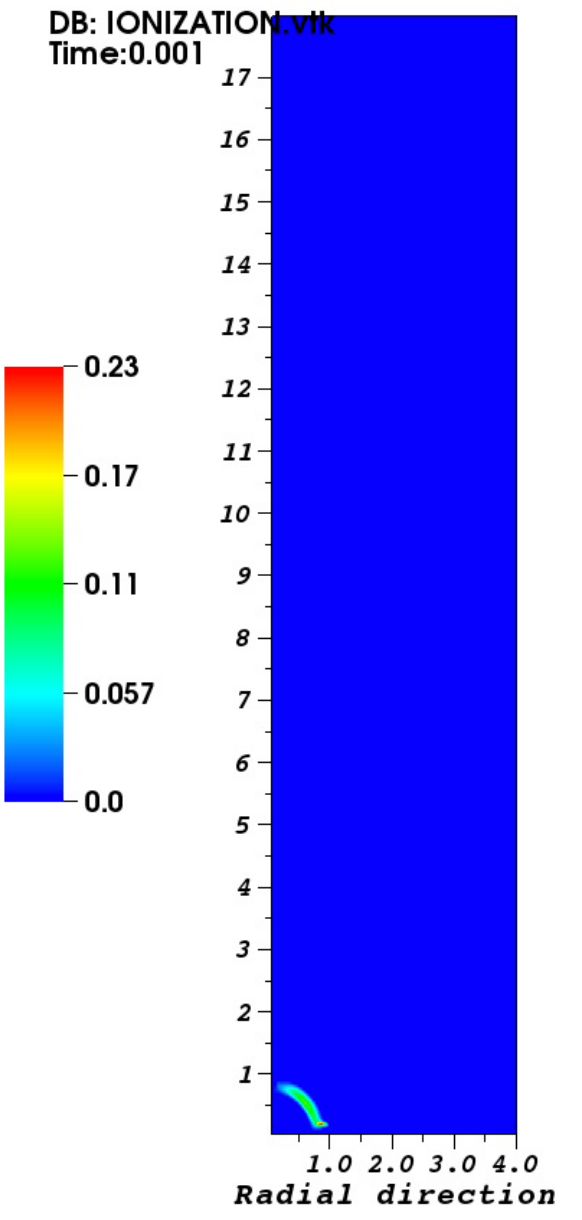

Density, Temperature, Average Ionization at 5 microsecond

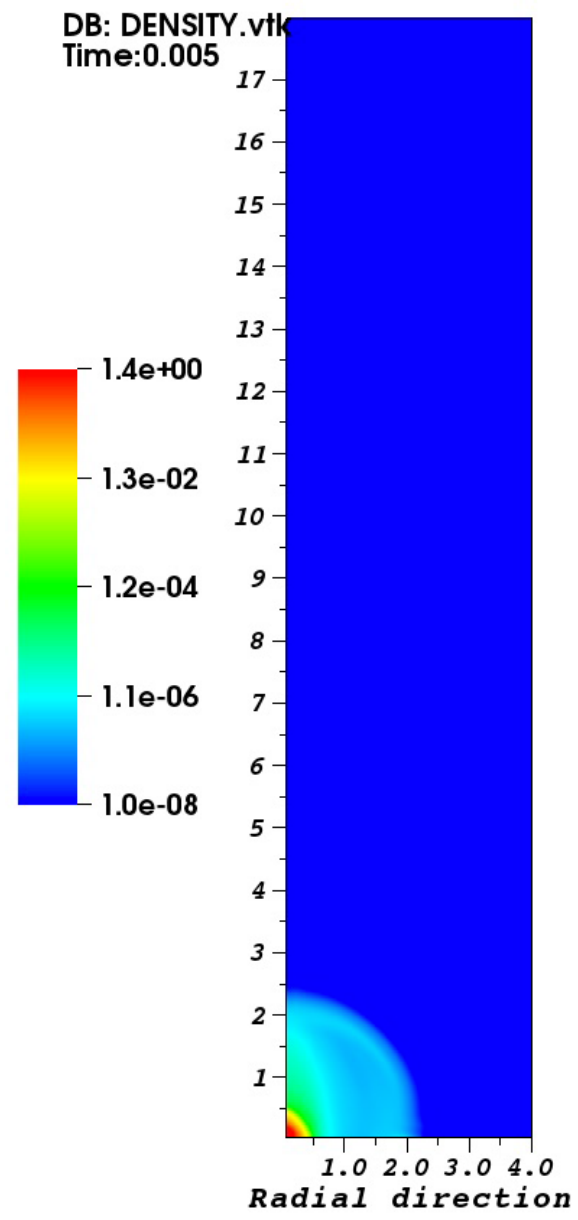

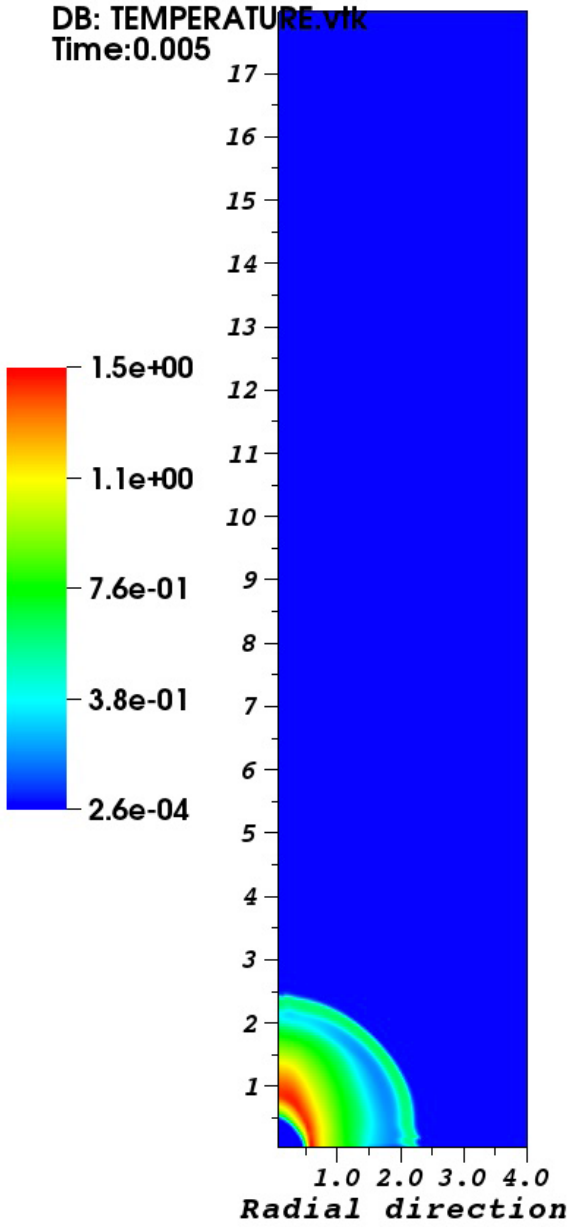

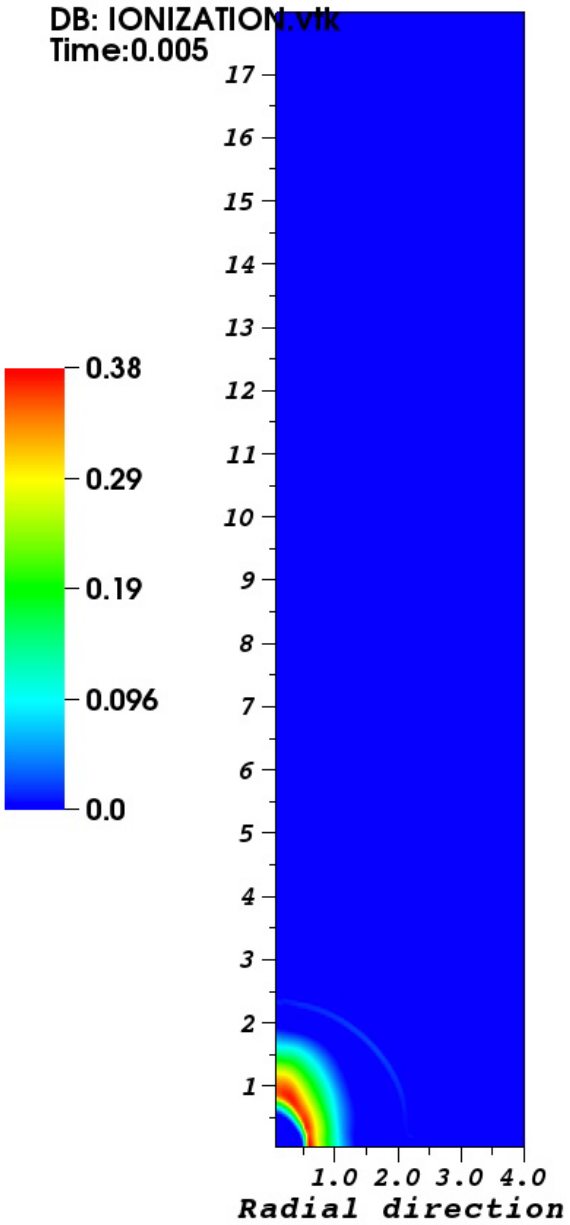

Density, Temperature, Average Ionization at 10 microsecond

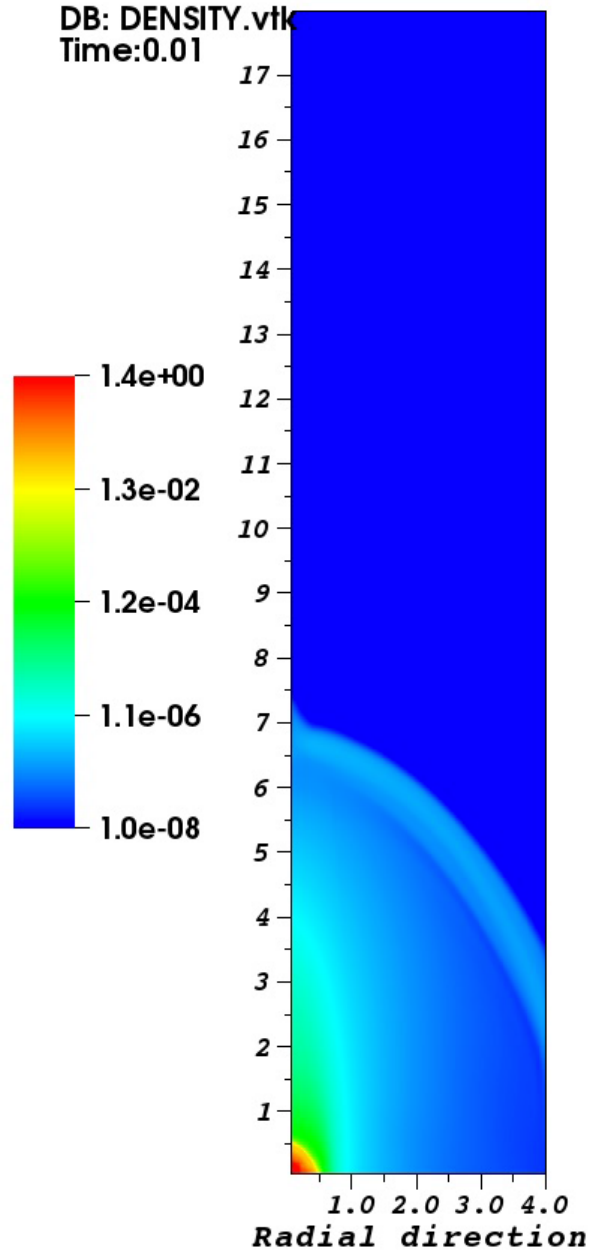

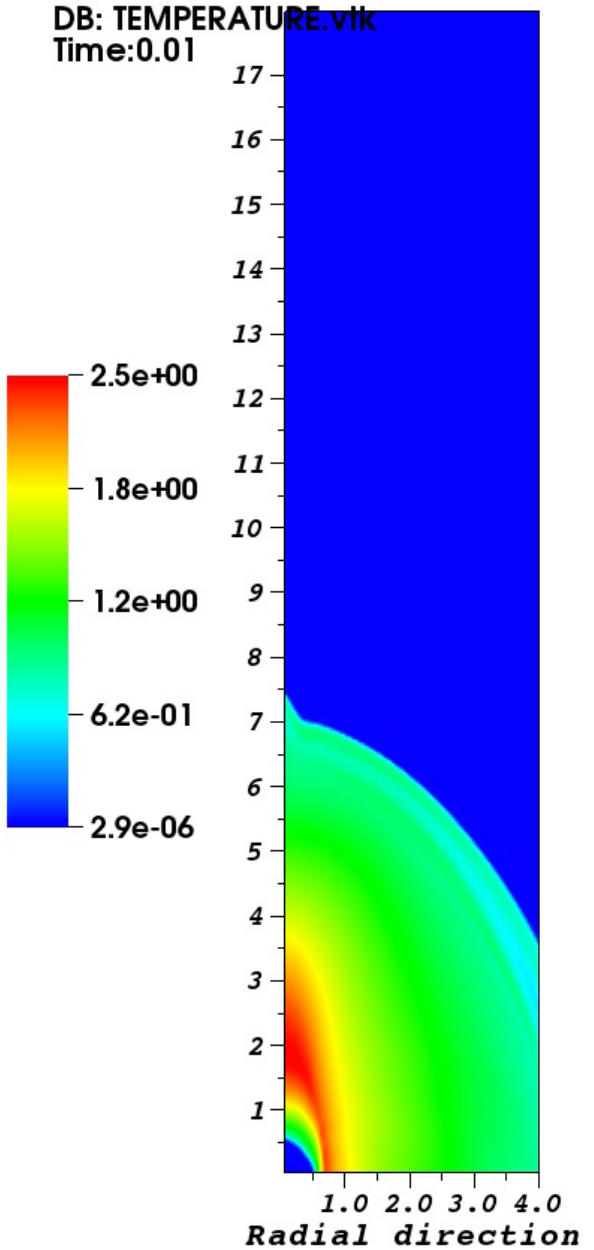

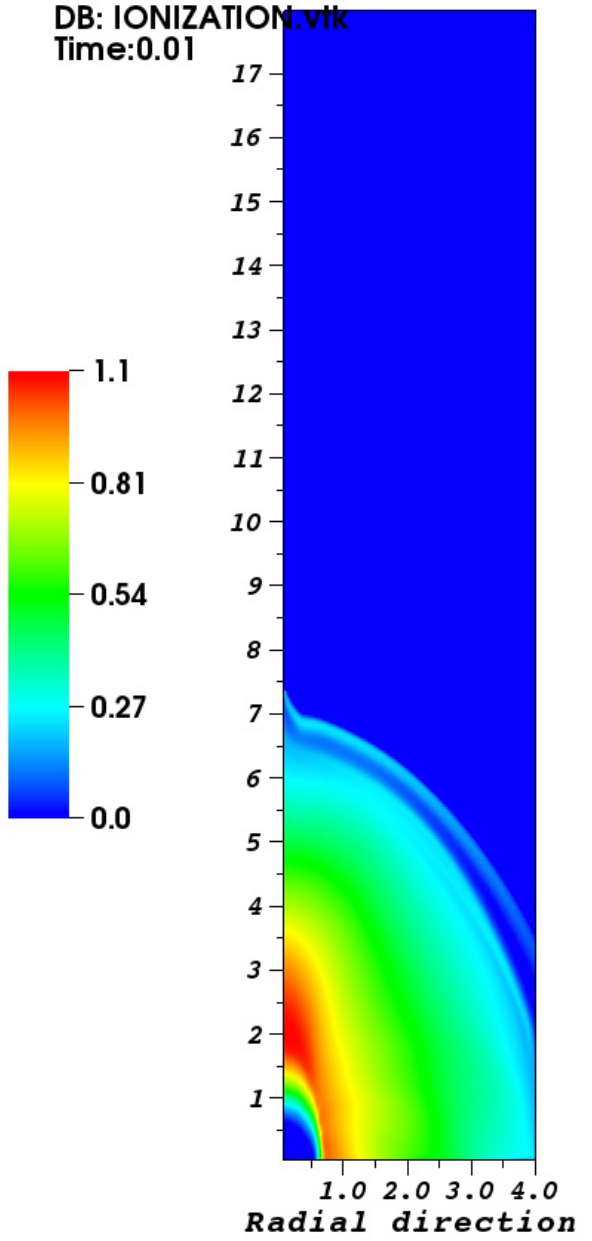

Density, Temperature, Average Ionization at 15 microsecond

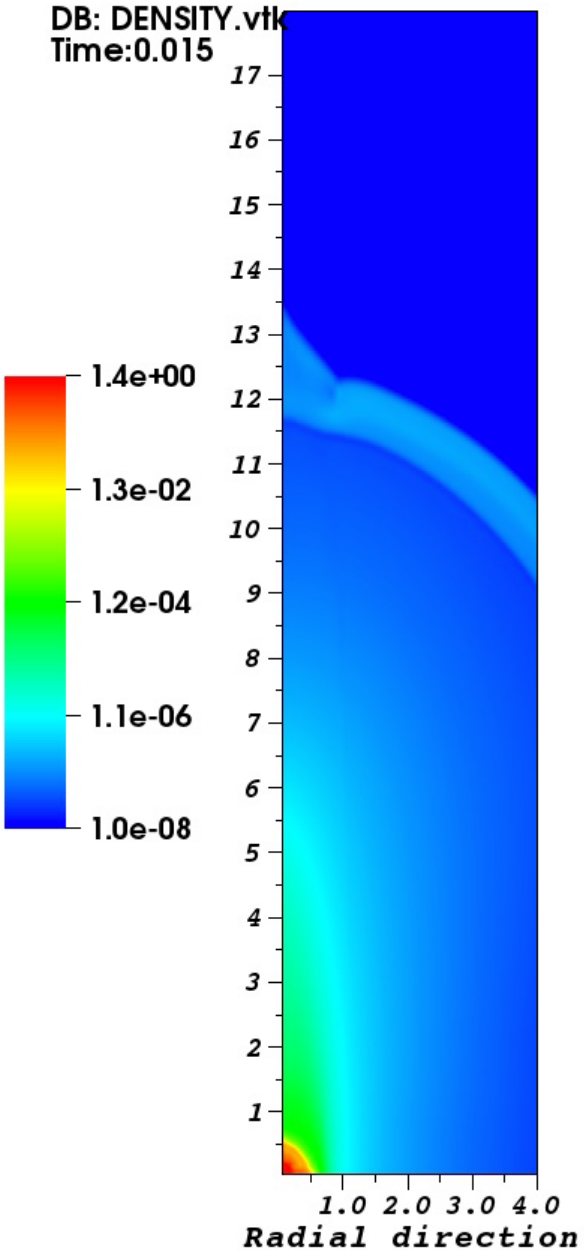

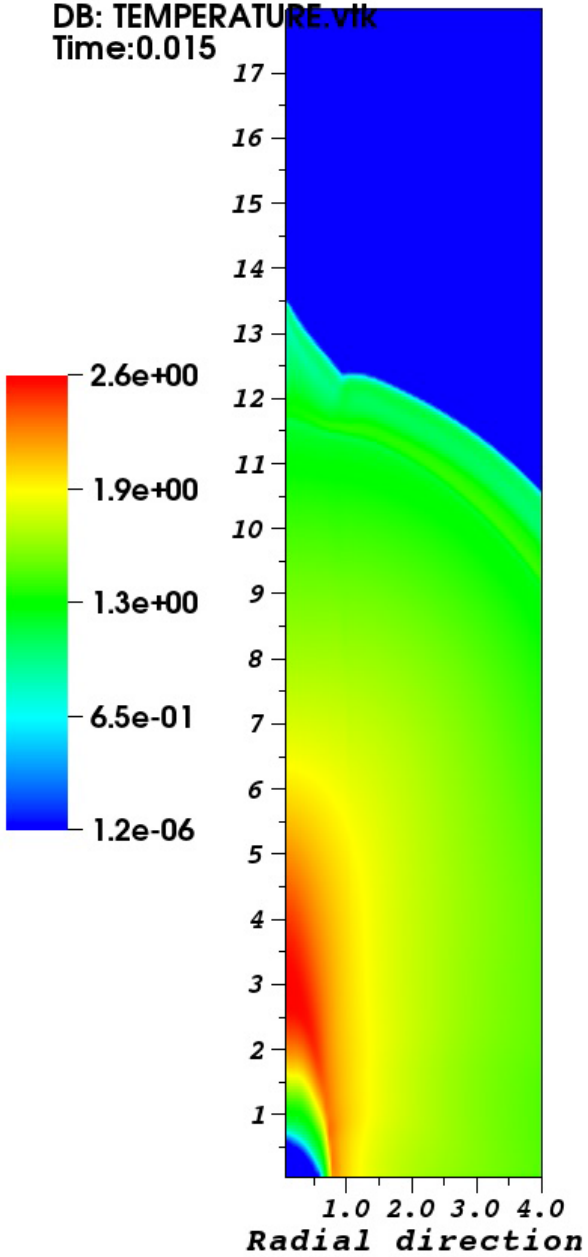

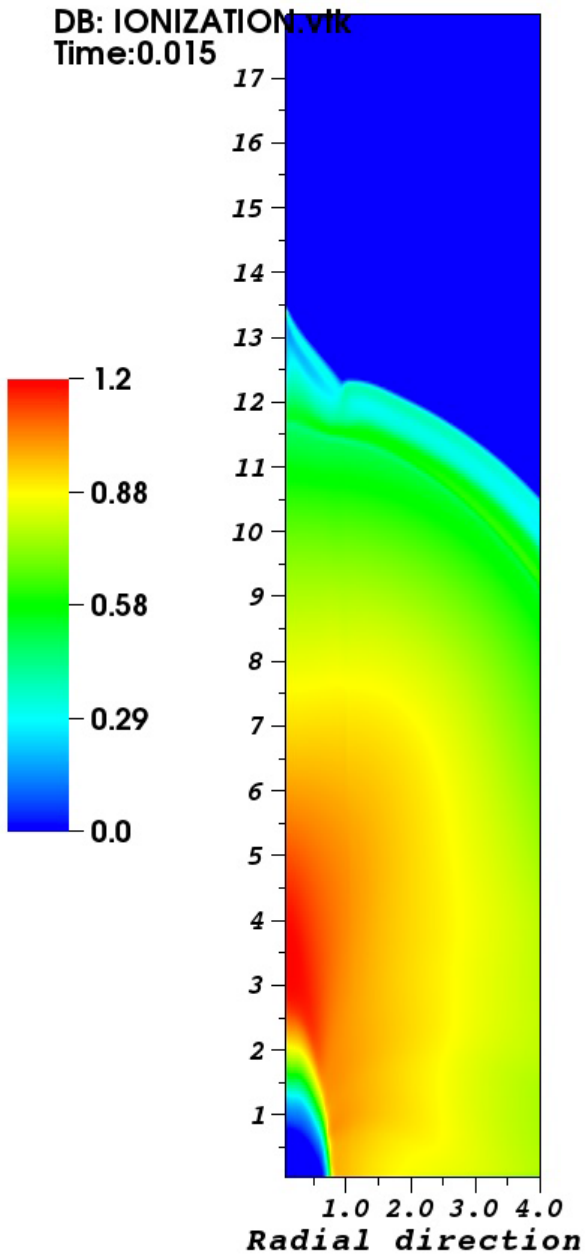

Density, Temperature, Average Ionization at 20 microsecond

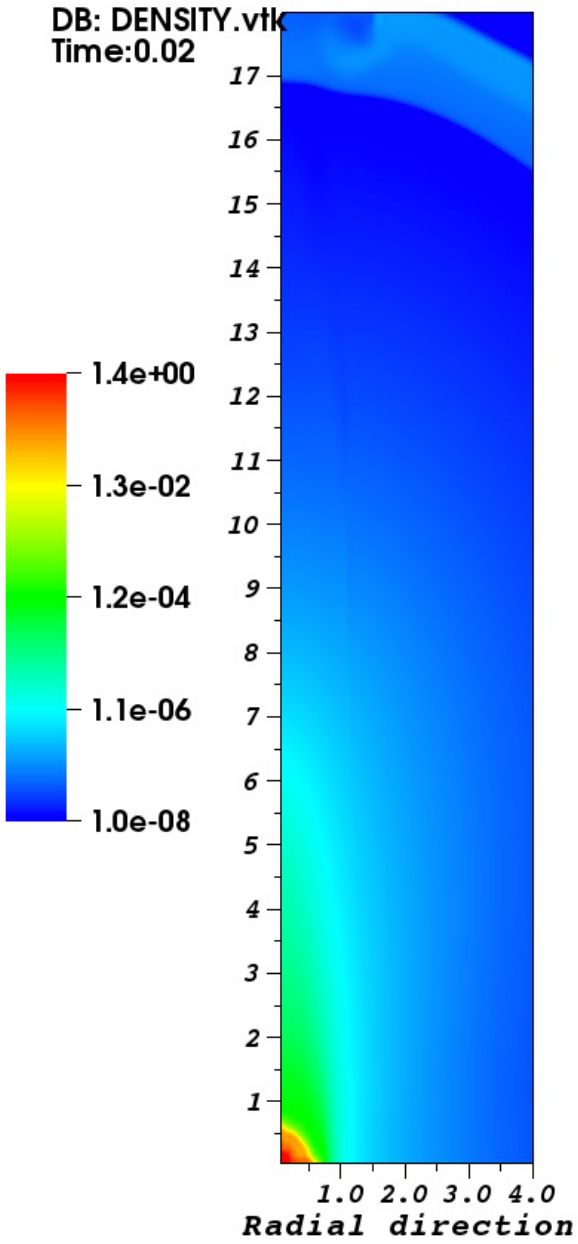

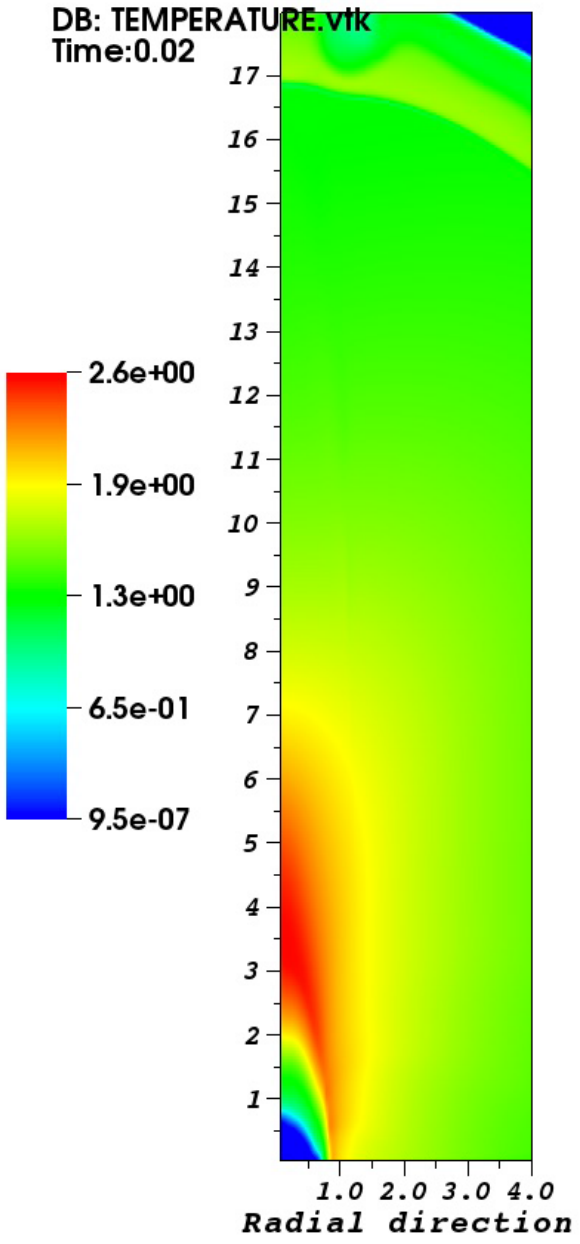

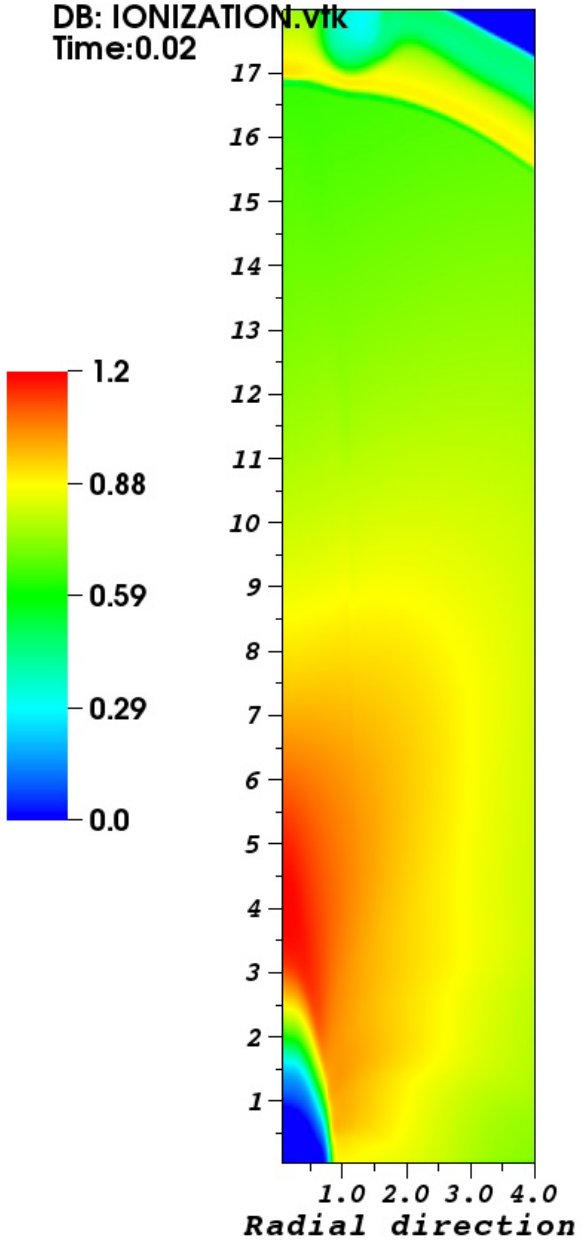

Density, Temperature, Average Ionization at 70 microsecond

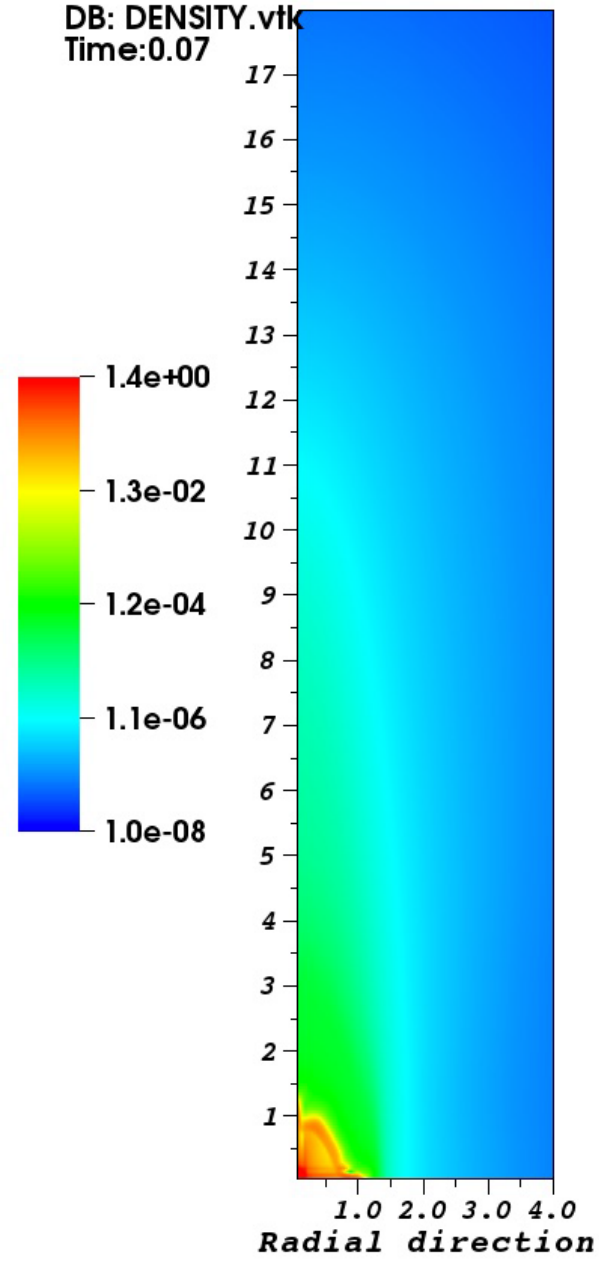

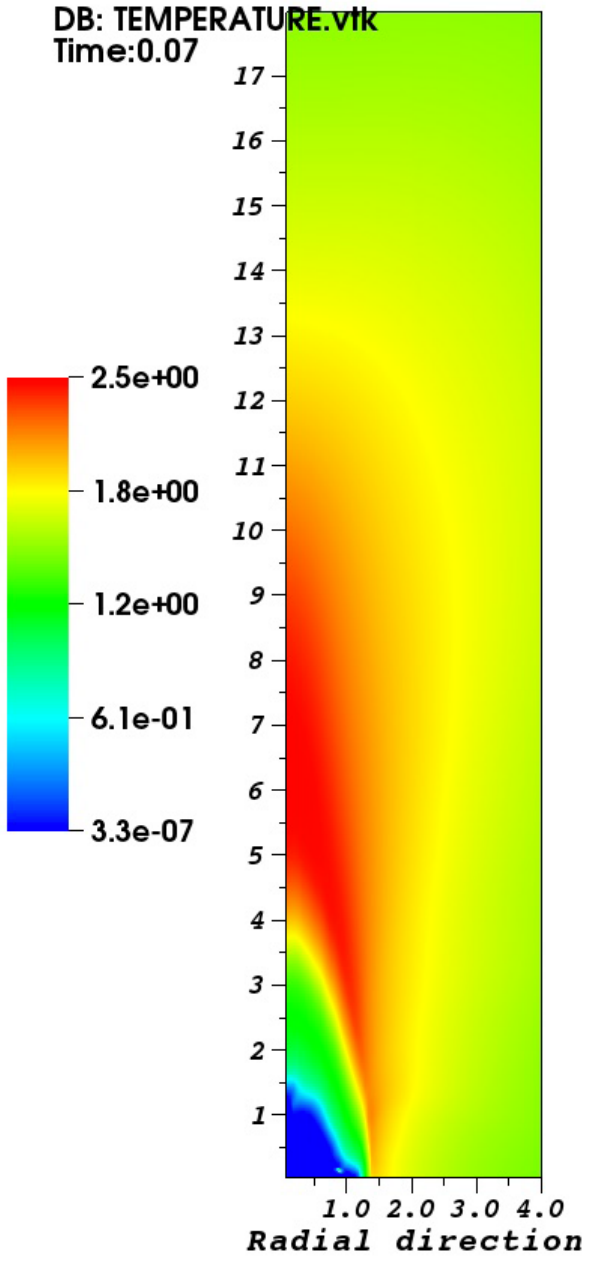

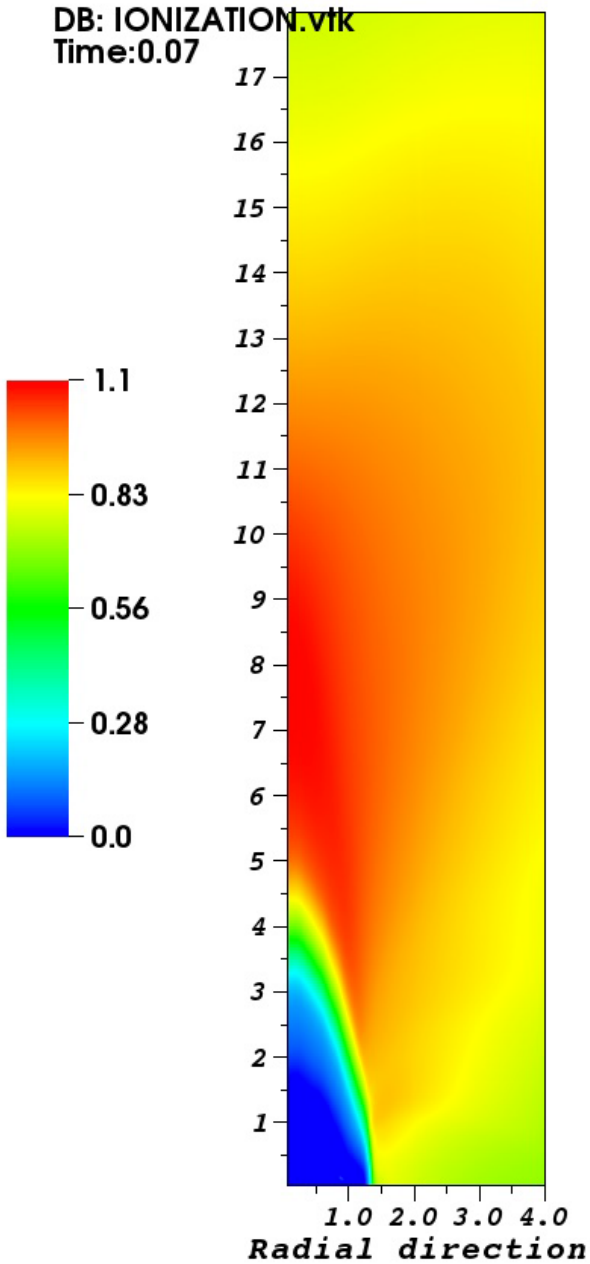

Pressure (bar) and Velocity (cm/ms = 10 m/s) at 20 microsecond

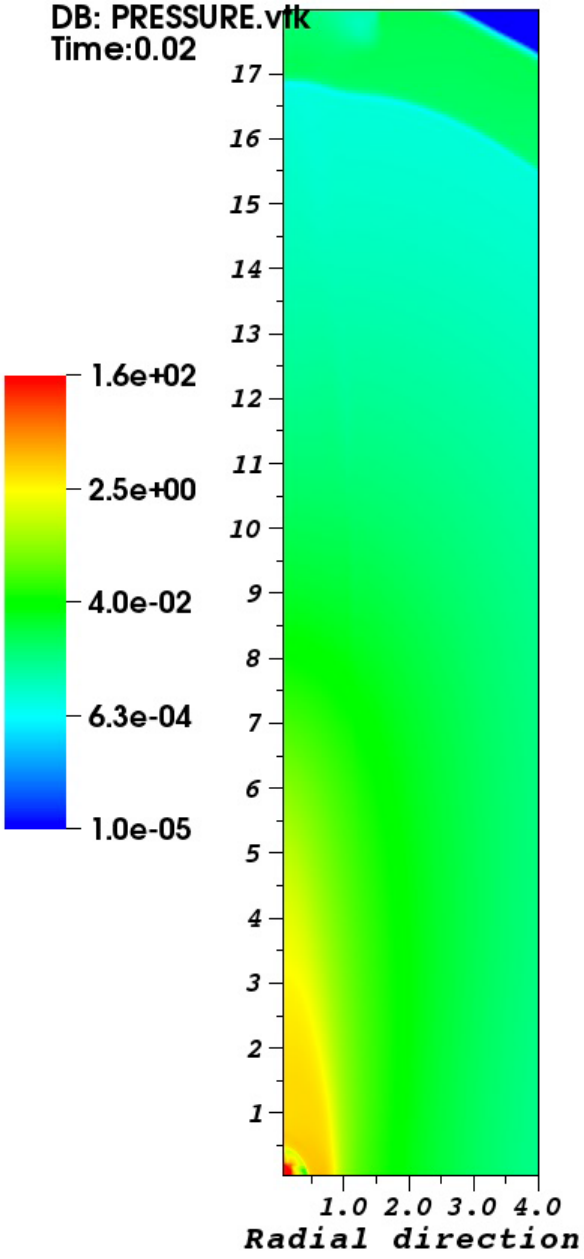

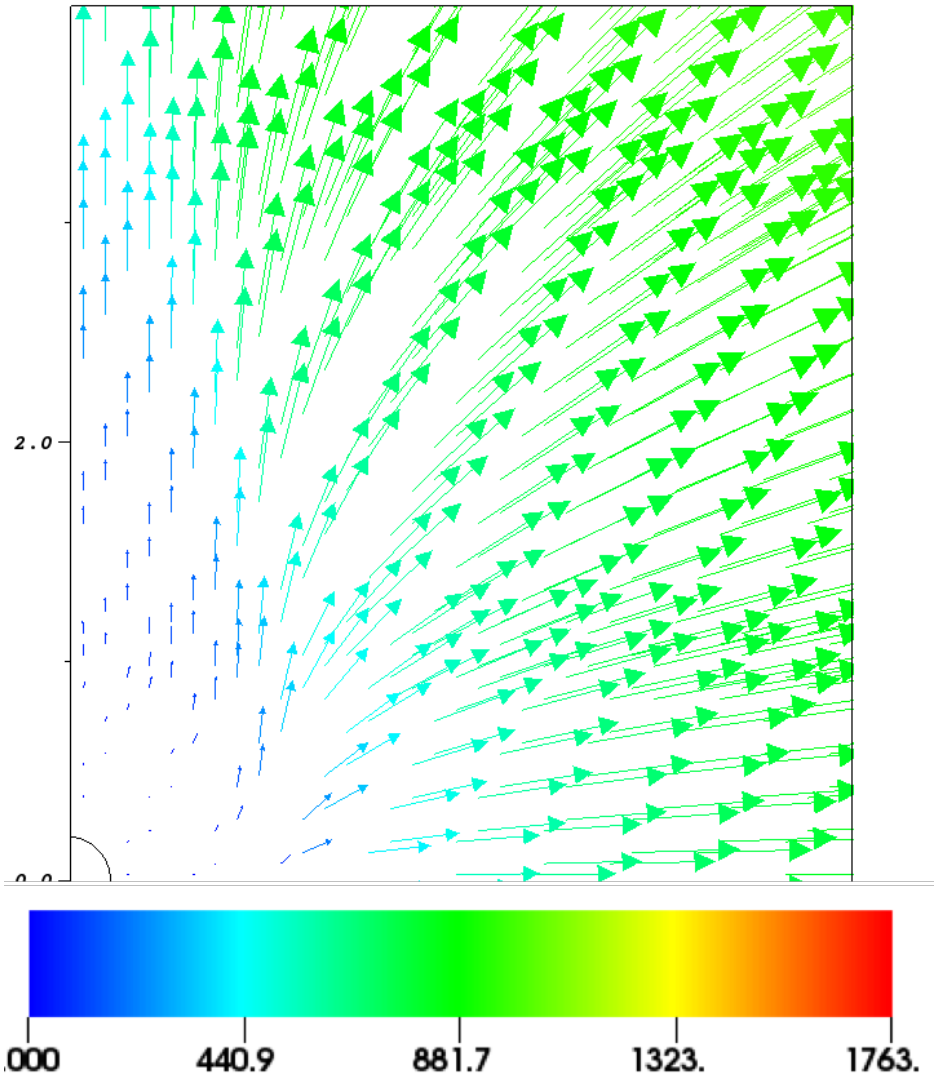

Density across and along the ablation channel

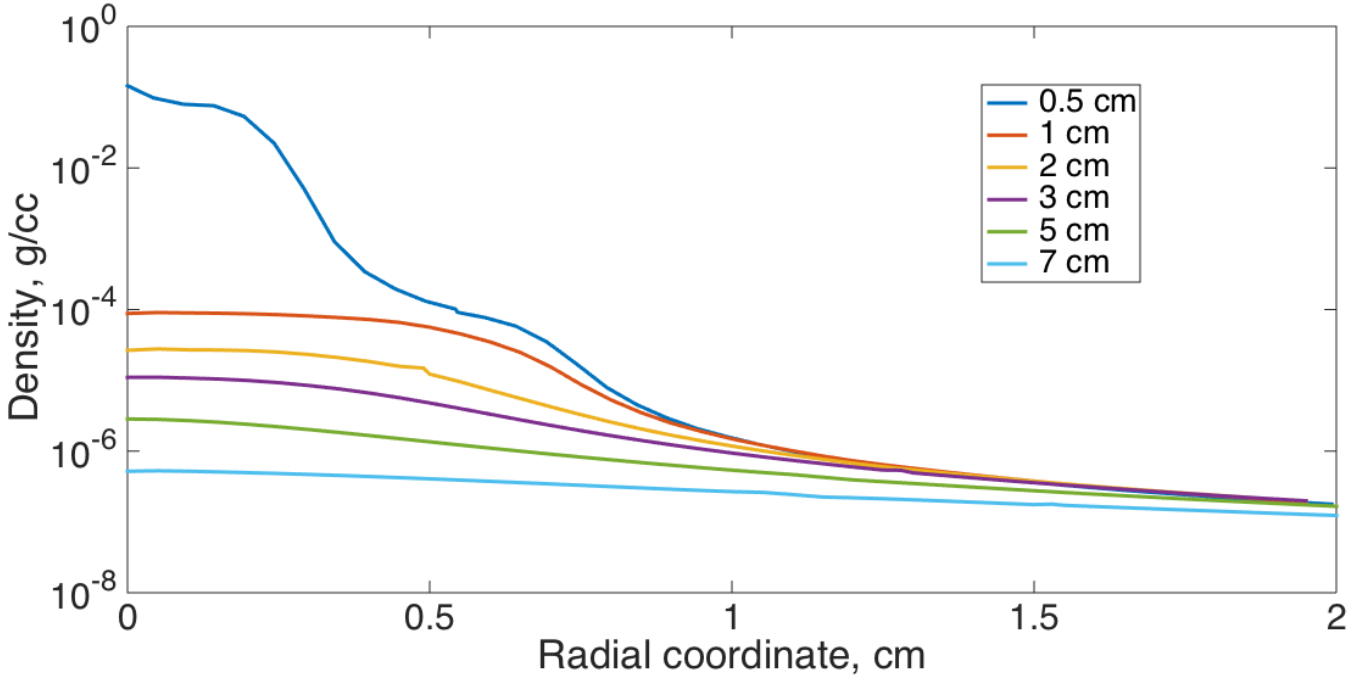

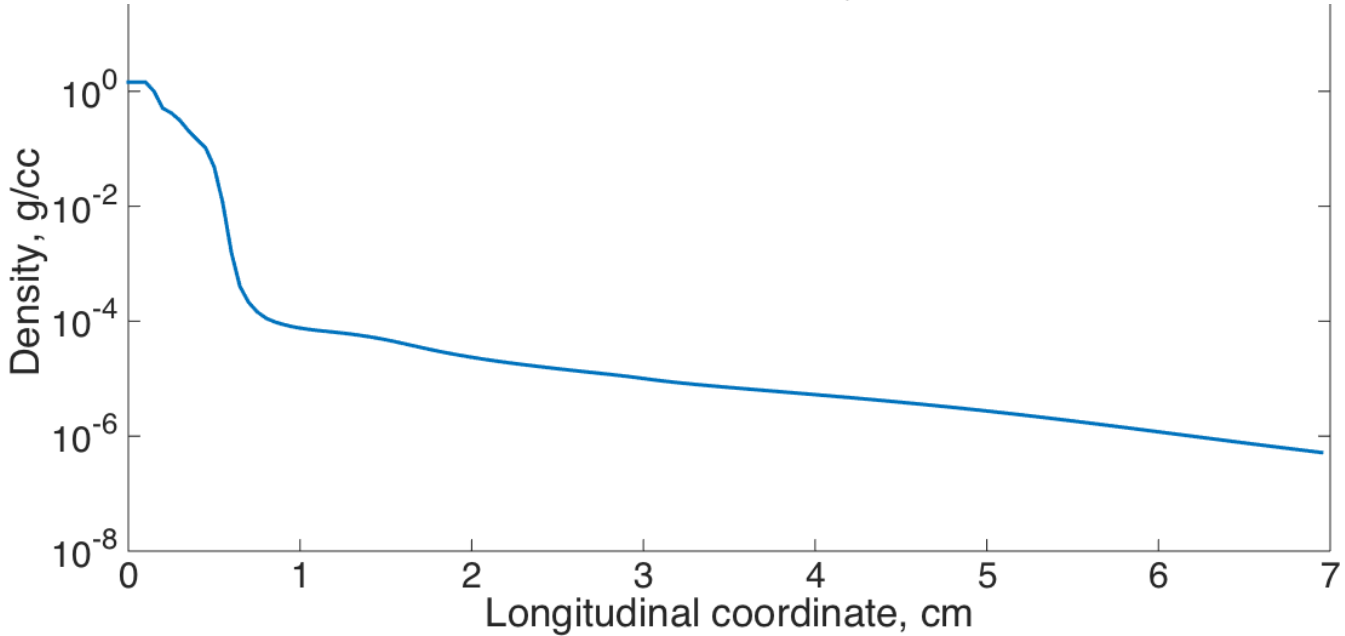

Temperature and Ionization across the ablation channel

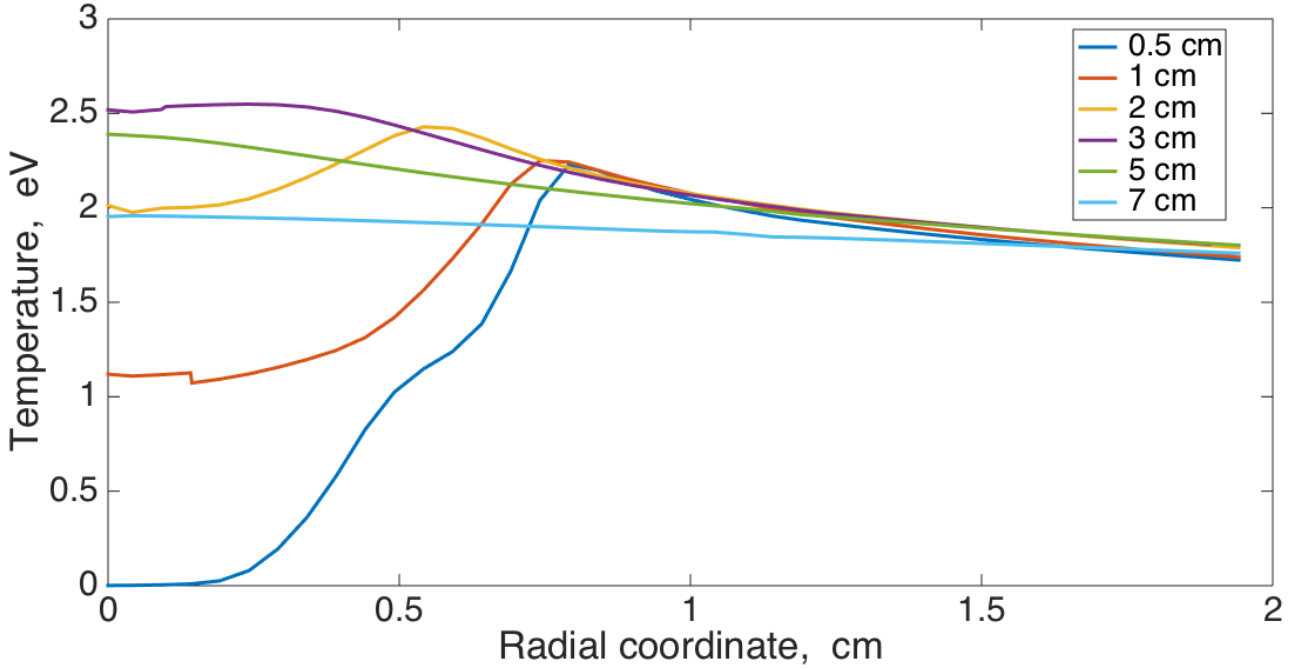

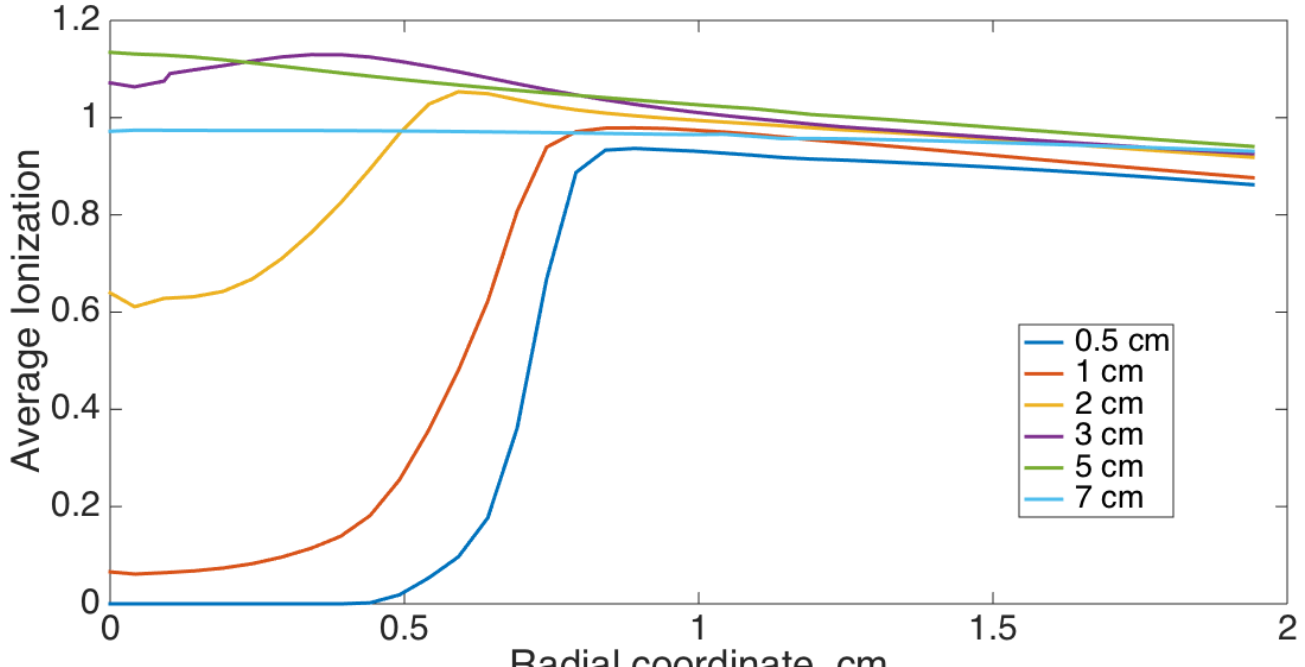

Effect of B field

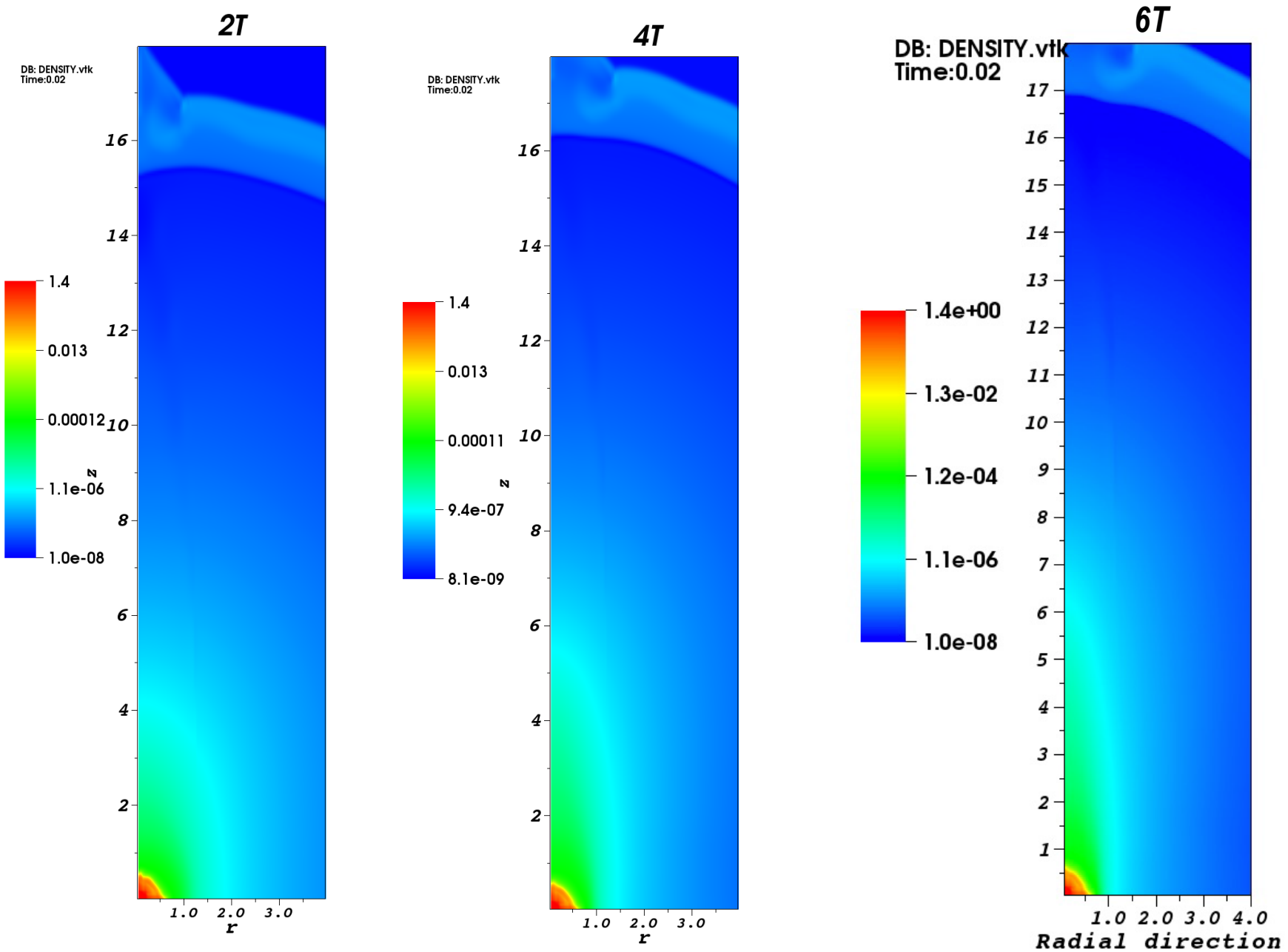

Effect of B field

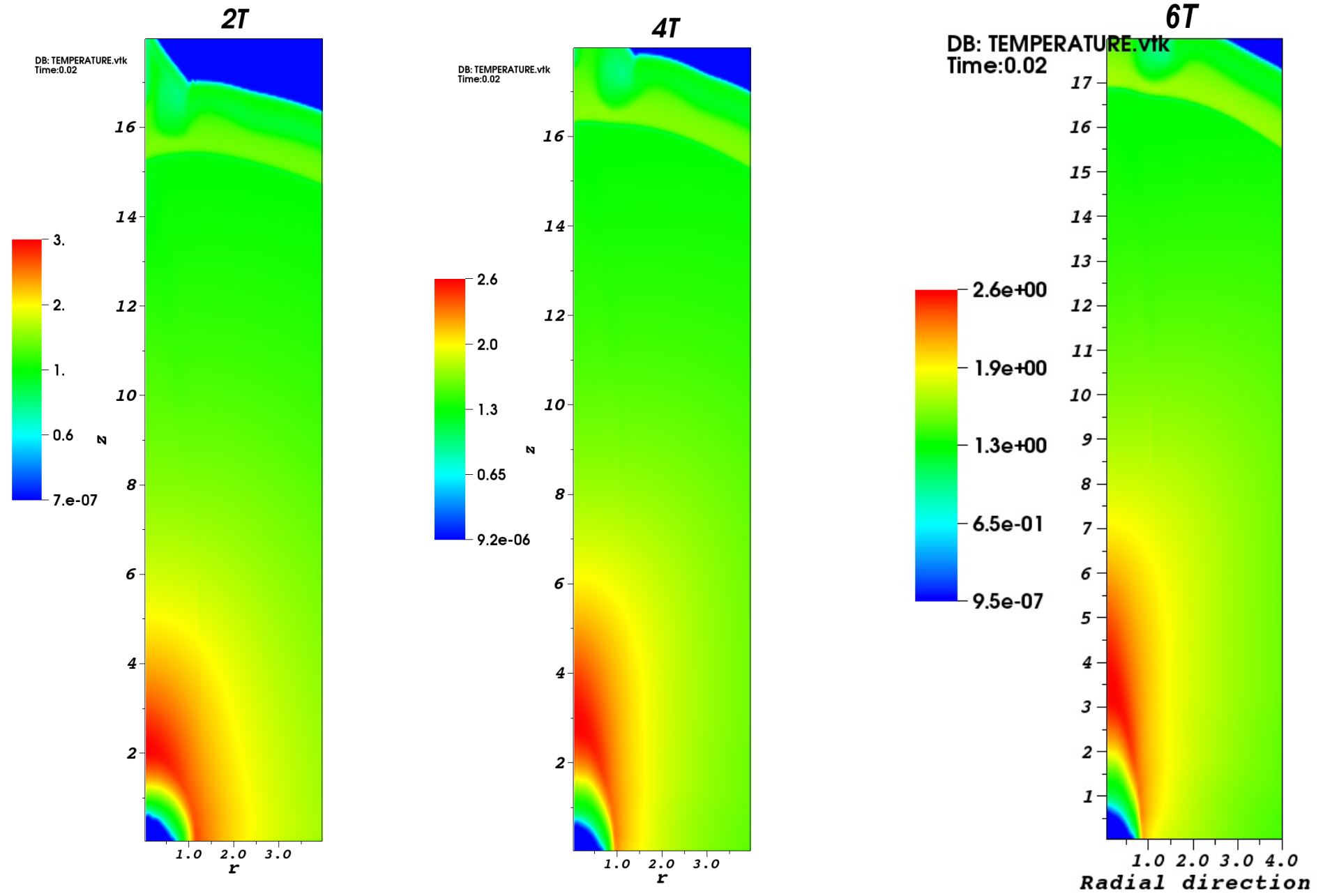

Effect of B field

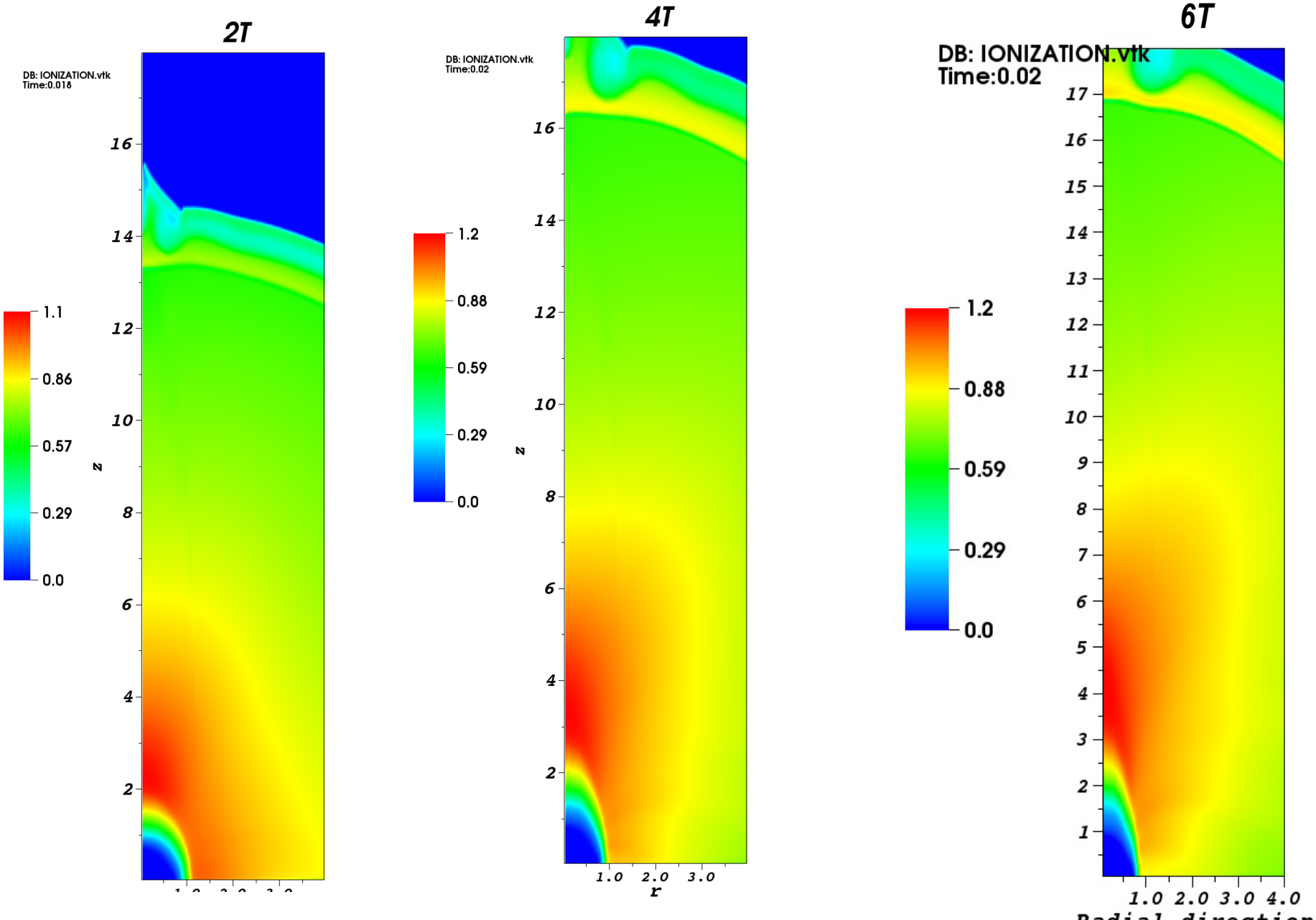

Models for SPI

Lagrangian Particles vs FronTier

- FronTier's main feature is the ability to track interfaces (ablation pellet surface, interface between ablated material and background plasma)
  - Tracking the ablated material interface is not beneficial
  - FronTier does not have AMR capabilities
    - Difficult to resolve large density gradients near the pellet in 2D (practically impossible in 3D)
  - FronTier must solve equations everywhere, including the background plasma
    - This "vacuum region" often leads to numerical instabilities

- An **optimal solution** to all outlined problems is the use of the **Lagrangian Particle Method**
  - Continuous adaptivity to density changes
  - Solve equations only for the ablated material, model the background (Lagrangian treatment of matter)
  - Interfaces of arbitrary complexity, stable and accurate solvers

Lagrangian Particle Method

Journal of Computational Physics

Available online 9 February 2018

In Press, Accepted Manuscript — Note to users

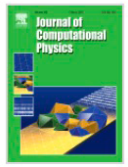

Lagrangian Particle Method for Compressible Fluid Dynamics

Roman Samulyak[a, b], Xingyu Wang[a], Hsin-Chiang Chen[a]

Show more

https://doi.org/10.1016/j.jcp.2018.02.004

Journal of Computational Physics 316 (2016) 682–699

Contents lists available at ScienceDirect

Journal of Computational Physics

www.elsevier.com/locate/jcp

AP-Cloud: Adaptive Particle-in-Cloud method for optimal solutions to Vlasov–Poisson equation

Xingyu Wang [a], Roman Samulyak [a,b,*], Xiangmin Jiao [a], Kwangmin Yu [a,b]

[a] Department of Applied Mathematics and Statistics, Stony Brook University, Stony Brook, NY 11794, United States
[b] Computational Science Initiative, Brookhaven National Laboratory, Upton, NY 11973, United States

Grid-based vs. Particle-based

- **Traditional methods:** Eulerian mesh-based PDE discretization with special algorithms for resolving interface (Volume-of-fluid, Level Set, Front tracking etc.)
  - Enhancement by various adaptive features (adaptive mesh refinement, AMR)
  - Require very complex meshes, potential loading balancing problems
  - Complexity causes potential difficulties in porting to new supercomputer architectures (GPU's, Intel-MIC's)

Particle-based (meshless) methods:

- Exact conservation (Lagrangian formalism)
- Capable of simulating extremely large non-uniform domains (natural, continuous adaptivity)
- Ability to robustly handle **material interfaces of any complexity**
- **Simplicity:** 3D code is not much more complex compared to a 1D code
- Bridge the gap between continuum and atomistic approaches

Motivation: Improvement of Accuracy and Convergence Order of SPH

• The main problem of traditional SPH (smooth particle hydrodynamics): very low accuracy of derivatives (zero-order, non-convergent), even for constant smoothing radius

- SPH derivative gives the similar accuracy to FD if particles are placed on rectangular mesh (due to cancellation of cross-terms)
- Accuracy rapidly decreases if particles even slightly deviate from the mesh
- The chain below is not based on rigorous approximation theory

$$A(\vec{r}) = \int A(\vec{r}')\,\delta(\vec{r}-\vec{r}')d\vec{r}' \longrightarrow A^W(\vec{r}) = \int A(\vec{r}')\,W(\vec{r}-\vec{r}',h)d\vec{r}'$$

$$A_i^W = \sum_j \frac{m_j}{\rho_j} A_j W_{ij}(h) \longrightarrow \nabla A_i^W$$

Stability of traditional SPH

- Traditional SPH is very stable. SPH code does not crash even if solutions develop into unphysical states
- Replacing SPH derivatives with very accurate GFD (generalized finite difference, or moving least squares) derivatives produces an unconditionally unstable code!
- Why bad derivatives lead to a stable discretization and accurate derivatives lead to an unstable scheme?
    - Inaccurate SPH discretization of Euler equations is identical to accurate Lagrange / Hamilton equations for the same particle system (interacting via isentropic potential energy)
    - Hamiltonian structure is responsible for the long term stability
    - Approximation of derivatives is related to linear errors

New Lagrangian Particle Method

- We keep only one idea of SPH: each particle represents a Lagrangian fluid cell
- Need to satisfy accuracy, stability, and efficiency on modern hardware

- Key novel features of our method:
    - Accuracy: derivatives based on generalized finite differences (optimal coefficients of a local stencil are found via least squares)
    - Stable particle-based upwind and directionally unsplit methods were designed
        - High order methods
    - Scalability on modern supercomputer architectures
- Complementary method: Adaptive Particle-in-Cloud (AP-Cloud). AP-Cloud is an adaptive and artifact-free replacement for the traditional PIC method

- The code is fully parallel (GPU version in progress)

Computing Derivatives.
Local Polynomial Fitting (Generalized Finite Differences)

- In 2D at the vicinity of a point 0, the function value in the location of a point i can be expressed as

$$U_i = U_0 + h_i \left.\frac{\partial U}{\partial x}\right|_0 + k_i \left.\frac{\partial U}{\partial y}\right|_0 + \frac{1}{2}\left(h_i^2 \left.\frac{\partial^2 U}{\partial x^2}\right|_0 + k_i^2 \left.\frac{\partial^2 U}{\partial y^2}\right|_0 + 2h_i k_i \left.\frac{\partial^2 U}{\partial x \partial y}\right|_0 \right) + \dots$$

- Second order approximation

$$\tilde{U} = U_0 + h_i\theta_1 + k_i\theta_2 + \frac{1}{2}h_i^2\theta_3 + \frac{1}{2}k_i^2\theta_4 + h_i k_i \theta_5$$

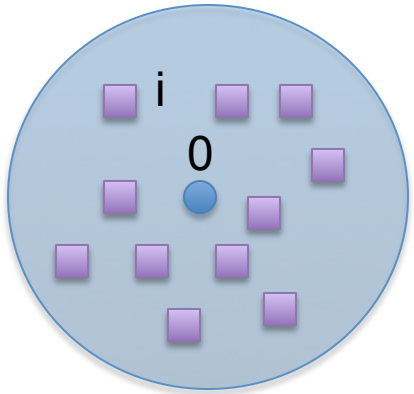

- Using *n* neighbours:

$$\begin{bmatrix} h_1 & k_1 & \frac{1}{2}h_1^2 & \frac{1}{2}k_1^2 & h_1k_1 \\ h_2 & k_2 & \frac{1}{2}h_2^2 & \frac{1}{2}k_2^2 & h_2k_2 \\ \vdots & \vdots & \vdots & \vdots & \vdots \\ h_n & k_n & \frac{1}{2}h_n^2 & \frac{1}{2}k_n^2 & h_nk_n \end{bmatrix} \begin{bmatrix} \theta_1 \\ \theta_2 \\ \theta_3 \\ \theta_4 \\ \theta_5 \end{bmatrix} = \begin{bmatrix} U_1 - U_0 \\ U_2 - U_0 \\ \vdots \\ U_n - U_0 \end{bmatrix}$$

Solve using QR to obtain derivatives **convergent to prescribed order**

Simulation Examples using Lagrangian Particles

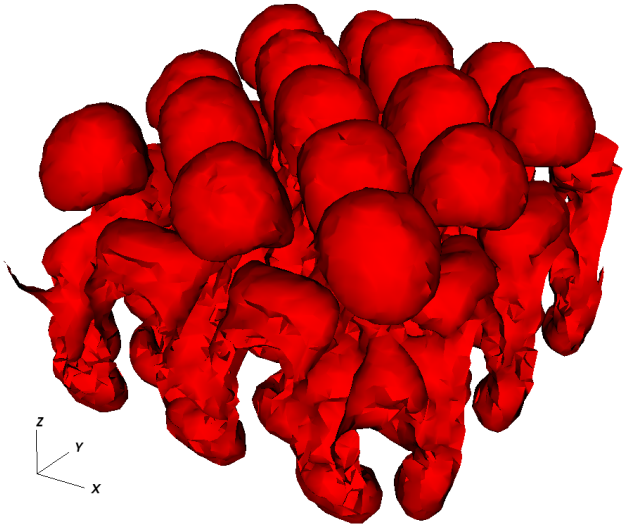

Rayleigh-Taylor Instability

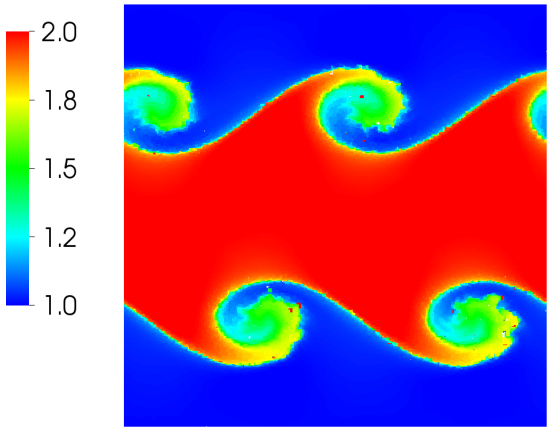

Kelvin-Helmholtz Instability

Triple-point Riemann problem
(producing shock, contact, vortex)

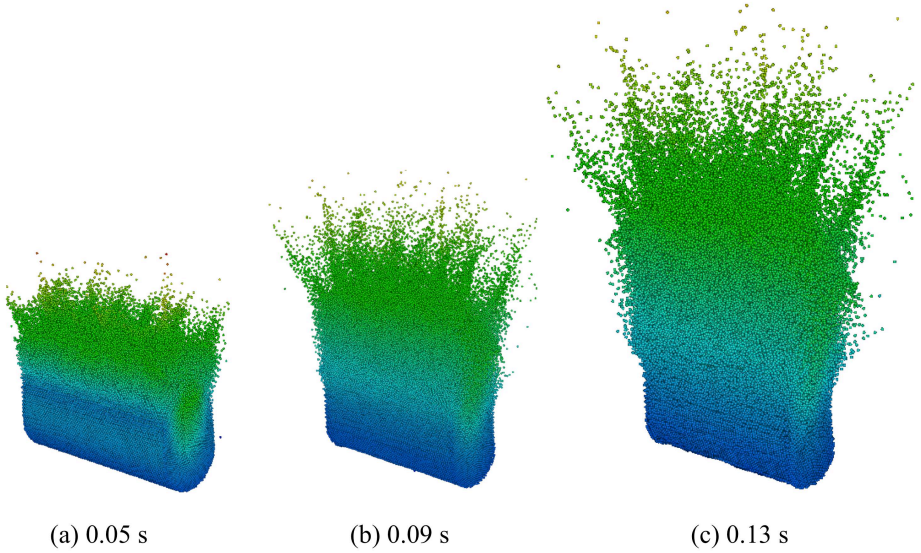

Splash of tungsten powder

CERN accelerator target prototype

Implementation of Pellet / SPI code based on Lagrangian Particles

- We have largely completed full 3D Lagrangian particle-based pellet code
- Kinetic models, phase transition models, radiation, EOS etc was ported from FronTier
- Only one new complex module: algorithm for line integrals of density
  - Task: In 2D, given N particles $p_i=(x_i, y_i)$, i={1,2,…,N}, calculate I_i, integral of density in (-inf, x_i) along line $y=y_i$.
  - Sort particles in x ascending order;
  - Divide the y domain into M cells C_j, j={1,2,…,M} with size dy. Initialize the S_j, integral in each cell to be zero;
  - Iterate over all particles. For each particle $p_i=(x_i,y_i)$, find the cell C_j containing y_i. $I_i=S_j$ will be the integral of density up to p_i. Add the contribution of p_i to S_j: $S_j=S_j+m_i/dy$, where m_i is the mass of p_i.
  - Cells data is stored in hash table data structure to avoid wasting memory for cells containing no particles.
  - 3D algorithm is similar

The density integral calculated on 5 pellet clouds. The integral direction is from right to left in x).

In the case of Poisson-Vlasov problems, with successfully worked with density changes by 3 – 5 orders of magnitude